

**ASSESSING THE INFLUENCE OF DIAGENESIS ON RESERVOIR
QUALITY: HAPPY SPRABERRY FIELD, GARZA COUNTY,
TEXAS**

A Thesis

by

VINCENT PHILIPPE GUILLAUME MAZINGUE-DESAILLY

Submitted to the Office of Graduate Studies of
Texas A&M University
in partial fulfillment of the requirements for the degree of

MASTER OF SCIENCE

May 2004

Major Subject: Geology

**ASSESSING THE INFLUENCE OF DIAGENESIS ON RESERVOIR
QUALITY: HAPPY SPRABERRY FIELD, GARZA COUNTY,
TEXAS**

A Thesis

by

VINCENT PHILIPPE GUILLAUME MAZINGUE-DESAILLY

Submitted to Texas A&M University
in partial fulfillment of the requirements
for the degree of

MASTER OF SCIENCE

Approved as to style and content by:

Wayne M. Ahr
(Chair of Committee)

Duane A. Mc Vay
(Member)

Brian J. Willis
(Member)

Richard L. Carlson
(Head of Department)

May 2004

Major Subject: Geology

ABSTRACT

Assessing the Influence of Diagenesis on Reservoir Quality:

Happy Spraberry Field, Garza County, Texas. (May 2004)

Vincent Philippe Guillaume Mazingue-Desailly, Dip., Ecole des Mines de Paris

Chair of Advisory Committee: Dr. Wayne M. Ahr

In the Permian Basin, strata of Leonardian age typically consist of interbedded carbonates and siliciclastics interpreted to be turbidite deposits. Happy Spraberry Field produces from a 100-foot thick carbonate section in the Lower Clear Fork Formation (Lower Leonardian) on the Eastern Shelf of the Midland Basin. Reservoir facies include oolitic- to-skeletal grainstones and packstones, rudstones and *in situ Tubiphytes* bindstones. Depositional environments vary from open marine reefs to shallow marine oolitic shoal mounds. Best reservoir rocks are found in the oolitic-skeletal packstones.

Diagenesis occurred in several phases and includes (1) micritization, (2) stabilization of skeletal fragments, (3) recrystallization of lime mud, (4) intense and selective dissolution, (5) precipitation of four different stages of calcite cement, (6) mechanical compaction, (7) late formation of anhydrite and (8) saddle dolomite and (9) replacement by chalcedony. Oomoldic porosity is the dominant pore type in oolitic grainstones and packstones. Incomplete dissolution of some ooids left ring-shaped structures that indicate ooids were originally bi-mineralic. Bacterial sulfate reduction is suggested by the presence of (1) dissolved anhydrite, (2) saddle dolomite, (3) late-stage coarse-calcite cement and (4) small clusters of pyrite.

Diagenetic overprinting on depositional porosity is clearly evident in all reservoir facies and is especially important in the less-cemented parts of the oolitic grainstones where partially-dissolved ooids were subjected to mechanical compaction resulting in “eggshell” remnants. Pore filling by late anhydrite is most extensive in zones where dissolution and compaction were intense.

Finally, a porosity-permeability model was constructed to present variations in oolitic packstone- rudstone-bindstone reservoir rocks. The poroperm model could not be applied to oolitic grainstone intervals because no consistent trends in the spatial distribution of porosity and permeability were identified. Routine core analysis did not produce any reliable value of water saturation (S_w). An attempt to take advantage of wireline log data indicates that the saturation exponent (n) may be variable in this reservoir.

ACKNOWLEDGMENTS

I wish to express my sincerest gratitude to Dr. Wayne M. Ahr, chair of my committee, who provided what I needed the most for this study: lots of explanations and enthusiasm. The time he gave me was very constructive and useful. He also provided all the dataset needed for this work.

I wish to thank my committee members: Dr. Brian J. Willis who provided a critical review for this paper, and Dr. Duane A. Mc Vay who brought an alternate vista from a petroleum-engineering standpoint. I would also like to thank Dr. Richard L. Carlson, head of the Geology department, and all the teachers I met at Texas A&M University. The time I spent in both the Geology and the Petroleum Engineering departments during this study and the classes I have taken have provided me with a great opportunity to complete my education.

I would like to thank Total who provided funding for this study and especially Dr. Herbert Eichenseer who was my tutor in that company.

I want to express thanks to Domenico and Aaron, students of the ground floor in the Geology department, who helped a lot the ignorant student I was about microscopes and petrographic description. I have special thanks for Ahmed; his support never failed.

TABLE OF CONTENTS

	Page
ABSTRACT	iii
ACKNOWLEDGMENTS.....	v
TABLE OF CONTENTS	vi
LIST OF FIGURES.....	viii
LIST OF TABLES	x
INTRODUCTION.....	1
Field location and history	3
REGIONAL GEOLOGIC SETTINGS	6
Structure	6
Stratigraphy.....	7
METHODS.....	11
Previous work.....	11
Available data.....	11
Nature of this study	13
LITHOFACIES AND DEPOSITIONAL ENVIRONMENT	14
Lithofacies.....	14
Depositional environment	22
Field geometry and well location	22
DIAGENESIS	25
Description of the diagenetic features.....	25
Effect of diagenesis on porosity	35
Thermosulfate reduction	39
Eggshell diagenesis	41
Analog studies.....	41

	Page
POROSITY, PERMEABILITY AND WATER SATURATION.....	48
Porosity-permeability correlations	48
Saturation exponent and fluids saturation	55
CONCLUSIONS.....	60
REFERENCES CITED.....	61
APPENDIX.....	65
VITA	69

LIST OF FIGURES

	Page
Figure 1. Field location map (modified after Atchley et al, 1999).....	2
Figure 2. Stratigraphic column for the Eastern Shelf and Midland Basin during Leonardian time.....	4
Figure 3. Base map of Happy Spraberry Field.....	5
Figure 4. Generalized stratigraphic cross section of the Midland Basin-Eastern Shelf transition.....	8
Figure 5. Shelf to basin stratigraphic correlation	10
Figure 6. Core photo of oolitic grainstone at 4933 feet, well Lott 19-4.....	15
Figure 7. Ring shaped structures left by selective dissolution within ooids	17
Figure 8. Core photo of rudstones and floatstones.....	19
Figure 9. Core photo of <i>Tubiphytes</i> bindstones.....	20
Figure 10. Core photo of siliciclastics.....	21
Figure 11. Structure map on top of the Happy Field carbonates.....	24
Figure 12. Thin section photograph showing isopachous circumgranular calcite cement colored by Alizarin Red S stain	26
Figure 13. Circumgranular isopachous cement and calcite cement I broken by compaction, from a sample at 4919.3 feet, well Lott 19-4.....	28
Figure 14. Effect of compaction from a sample at 4926.9 feet, well Lott 19-4	30
Figure 15. Calcite cement II from a sample at 4919.3 feet, well Lott 19-4	32
Figure 16. Calcite cement III from a sample at 4981.5 feet, well Lott 19-8.....	33
Figure 17. Anhydrite from a sample at 4933.1 feet, well Lott 19-4.....	34
Figure 18. Saddle dolomite from a sample at 4960.6 feet, well Lott 19-4.....	36
Figure 19. Chalcedony replacement from a sample at 4982.2 feet, well Lott 19-8	37

	Page
Figure 20. Diagrammatic summary of diagenetic environments at Happy Spraberry Field.....	38
Figure 21. Study of the Southwest Andrews area	43
Figure 22. Highly schematic west-east cross sections throughout the Delaware and Midland Basins.....	46
Figure 23. Well 19-7. Porosity-permeability semi-log cross plot.....	50
Figure 24. Well 19-8. Porosity-permeability semi-log cross plot.....	51
Figure 25. Well 19-4. Porosity-permeability semi-log cross plot.....	52
Figure 26. Porosity-permeability semi-log cross plot that groups all rudstone, bindstone and oolitic packstone facies of wells Lott 19-4, Lott 19-7 and Lott 19-8	54
Figure 27. Effect of separate vug porosity on Archie “m”, or cementation exponent ...	57

LIST OF TABLES

	Page
Table 1. Data available in the studied wells.....	12
Table 2. Apparent water resistivity computed in wells Lott 19-4, Lott 19-7 and Lott 19-8.....	57
Table 3. Computation of the saturation exponent “n”, given initial water saturation....	59

INTRODUCTION

Estimates of hydrocarbon recovery over time depend on accurate knowledge of three main reservoir parameters: porosity, permeability and hydrocarbon saturation. Estimates of ultimate recovery follow directly from assessments of reservoir quality. In this study, reservoir quality is defined as the combined value of porosity and permeability; good reservoir quality corresponds to good values of both porosity and permeability and low reservoir quality to poor values of both porosity and permeability. Field development requires accurate models of porosity, permeability and oil saturation throughout the reservoir. Construction of such models is a difficult task because predictions must be interpolated from small samples of the reservoir. Cores are usually rare or they may not be available; consequently, many of the reservoir quality estimates must be made from well logs. Although well logs provide a fairly reliable estimate of porosity, they are less reliable as indicators of permeability. Permeability estimates from well logs can be improved by understanding primary and diagenetic mechanisms that control reservoir properties observed in core. This allows an evaluation of the degree and type of relationship between porosity and permeability. If there is a strong correlation between these parameters, then permeability can be estimated from log- derived porosity.

Unlike sandstone reservoir quality, which generally depends on the depositional distribution of grain size and only secondarily on pore-reducing diagenetic changes (e.g., physical compaction and cementation), limestone reservoirs are mineralogically unstable and mechanically less durable. Limestones can undergo many different types of diagenetic changes both soon after deposition and during longer term burial (Tucker, 1990; Moore, 2001). The effect of diagenesis on reservoir quality can be dramatic, completely overprinting depositional textures and fabrics.

This thesis follows the style and format of the American Association of Petroleum Geologists Bulletin.

Diagenetic overprints on depositional porosity are pronounced in the Clear Fork carbonates of the study area. (figure 1). This study is aimed at understanding how those diagenetic processes affected depositional reservoir characteristics in order to construct a poroperm model of the Happy Spraberry reservoir.

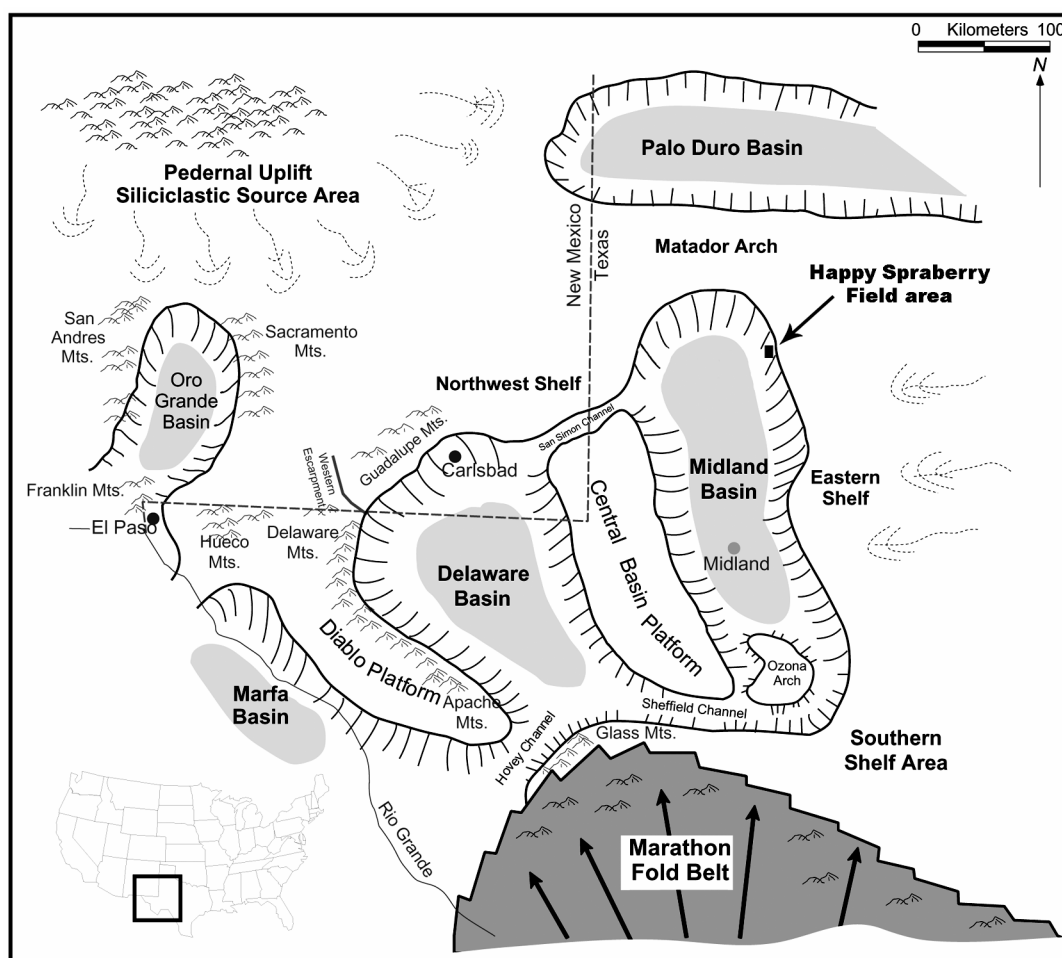


Figure 1. Field location map (modified after Atchley et al, 1999).

Field location and history

Happy Spraberry Field is located on the Eastern Shelf of the Permian Basin in Section 19, Block 2, T. & N.O.R.R. Co. Survey, Garza County, Texas. It produces from an interval about 100 feet thick at a depth of 5,000 feet. Though “Spraberry” is included in the field name, it does not produce from the Spraberry Formation, but from the Lower Clear Fork Formation of Lower Leonardian (Early Permian) age (figure 2). The field is about 0.6 square miles (1.6 square kilometers) and is penetrated by 15 wells (figure 3) that produce from oolitic skeletal grainstones, packstones, rudstones and bindstones.

Happy Spraberry Field was discovered in 1988 by Bennett Petroleum and field development began in 1989 under a joint venture with Torch Energy. Torch Operating Company has produced the field alone since 1991. A water flood program began in April 1992, but only small increases in both oil and water production rates were obtained. These low rates and volumes of recovered fluids do not account for the much larger volumes of injected water nor do they explain why the reservoir pressure has remained relatively static over time. This unexpected behavior suggests that a lack of communication exists between individual flow units and thus Happy Spraberry Field is a true compartmentalized reservoir.

		EASTERN SHELF	MIDLAND BASIN
Leonardian	Upper Leonardian	Upper Clear Fork	Spraberry (sandstones and carbonates)
		Middle Clear Fork	
	Lower Leonardian	Tubb Sandstone	Dean Sandstone
		Lower Clear Fork	Lower Leonardian (carbonates and shales)
		Wichita	

Figure 2. Stratigraphic column for the Eastern Shelf and Midland Basin during Leonardian time.

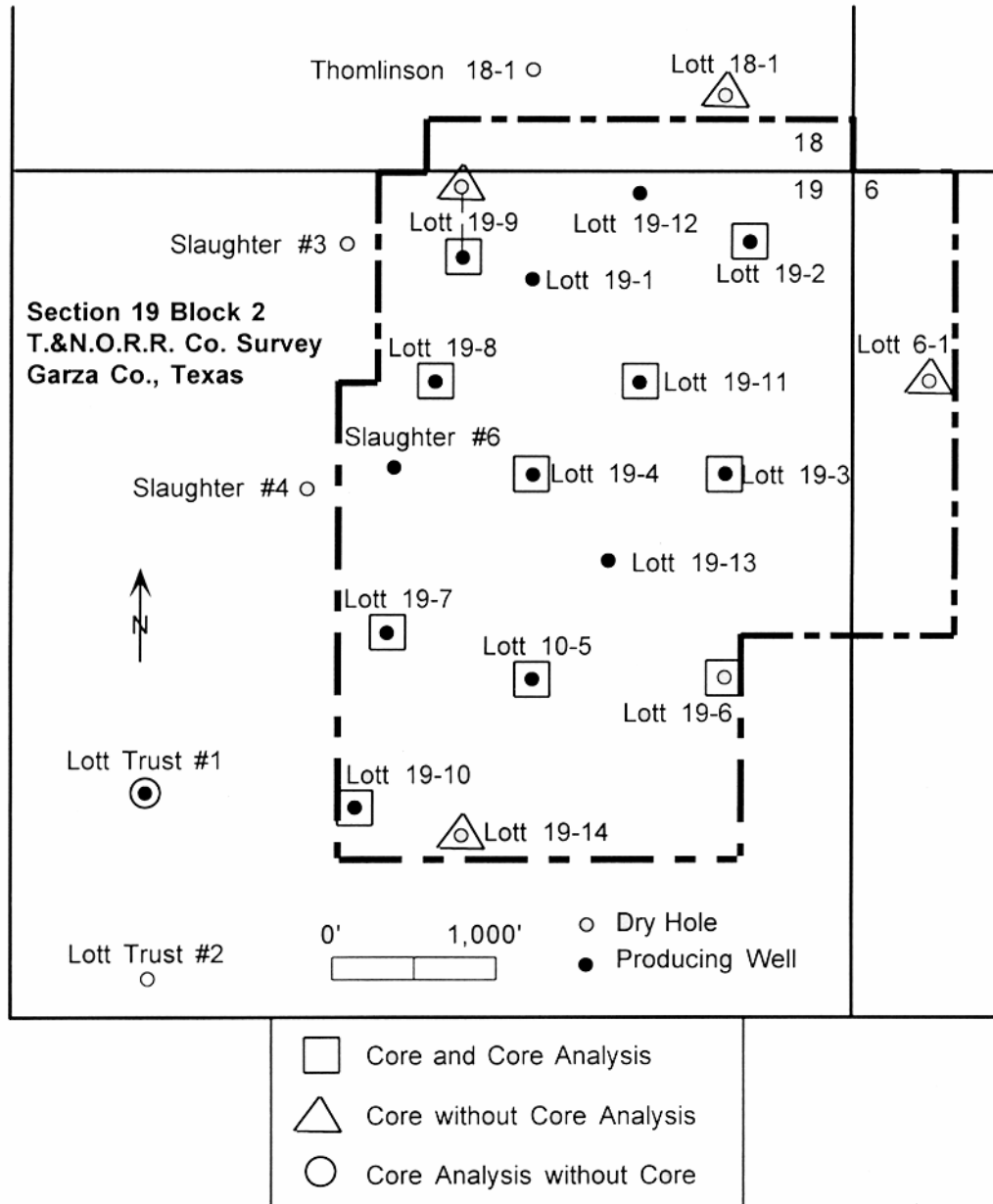


Figure 3. Base map of Happy Spraberry Field.

REGIONAL GEOLOGIC SETTINGS

Structure

The Permian Basin is an asymmetrical structural depression in the Precambrian basement of the North American plate. It covers about 115,000 square miles (300,000 square kilometers) in parts of West Texas and Southeastern New Mexico. The paleogeographic evolution of the Permian Basin is closely related to the breakup of the supercontinent Pangaea and subsequent late Paleozoic continental reassembly (Hills, 1985). Passive marginal structural elements formed in the early Paleozoic were reactivated as a series of foreland uplifts and intervening grabens during the late Paleozoic Marathon-Ouachita collision (Ross, 1986; Ward et al., 1986). The Midland Basin is bounded to the West by the Central Basin Platform, the main high of the Permian Basin, and to the East by the Chadbourne Fault zone. This fault zone corresponds to the transition from marine platform facies of the Eastern Shelf to the basinal facies of Midland Basin. The area marks the inflexion point of the shelf margin (Yang and Dorobek, 1994). Since Early Permian time, there has been little deformation of the Permian Basin (Mazzullo 1995) other than tilting along its edge during the Triassic (Ward et al., 1986; Mazzullo, 1995).

During Leonardian time, the Midland Basin was inundated by a tropical ocean. (Guevera, 1988). Depositional facies on the shelf included both siliciclastics and carbonates. Siliciclastic turbidites and density currents derived from the top of the shelf bypassed the shelf margin and passed into the basin (Ward et al., 1986). The Eastern Shelf of the Midland Basin was a distally-steepened ramp rather than a rimmed or open shelf. Happy Spraberry Field carbonates were deposited just inboard of this distally steepened margin (Hammel, 1996).

Stratigraphy

During Early Pennsylvanian time there was little input of terrigenous clastic sediment to Midland Basin and reef-like buildups developed. Some of these buildups, such as the Horseshoe Atoll, became major hydrocarbon reservoirs (Adams et al., 1951). Late Pennsylvanian time was a period of intense tectonic activity during the Ouachita-Marathon orogeny and widespread siliciclastic sedimentation (Yang and Dorobek, 1994). During Early Permian time, carbonate platforms developed around the edges of Midland Basin. By Early Leonardian time, reefs and mounds had formed along the western edge of the Eastern Shelf that were bypassed by siliciclastic turbidites being shed into the basin (Ward et al., 1986). As a result of this bypass sedimentation, Lower Clear Fork strata commonly consist of mixed, isolated biohermal buildups, oolitic sandbodies, discontinuous fluvial-deltaic arkosic sandstones and marine shales (Montgomery and Dixon, 1998). The Lower Clear Fork Formation (see figure 4) is considered to be time equivalent to the Dean Formation of Midland Basin (Handford, 1981).

Influx of siliciclastics into Midland Basin increased throughout Upper Leonardian times. Well established carbonate deposition along the platform margin of the Eastern Shelf continued to prograde westward. By the end of Leonardian times the Eastern Shelf had prograded as much as 24 km into Midland Basin (Mazzullo and Reid, 1989).

Middle and Upper Permian strata contain a sequence of, from base to top, carbonates, evaporites, and very fine arkosic sandstones and siltstones that are the fluvial, deltaic and lacustrine deposits of the Triassic Dockum Group and the Neogene Ogallala Formation (Stueber et al., 1998).

Stratigraphic correlation between units on the Eastern Shelf and those in Midland Basin strata is difficult because vertical relief between coeval beds on the platform top and the basin floor is on the order of 2,000 feet. The difficulty is exacerbated by facies

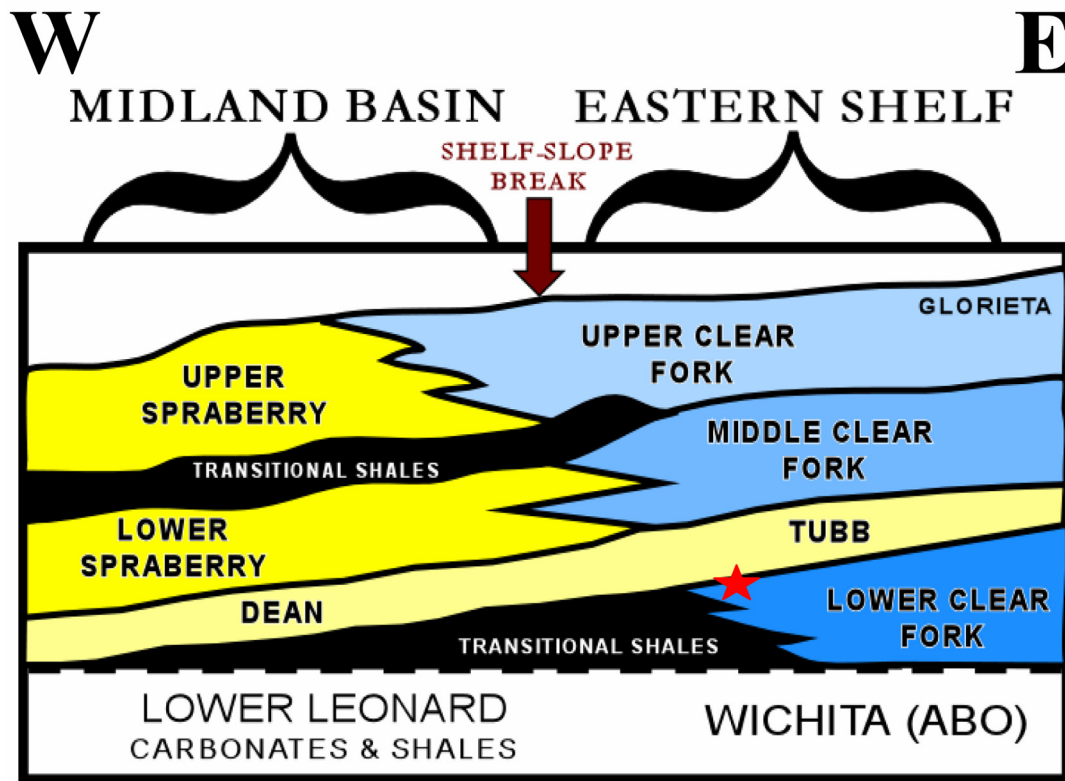


Figure 4. Generalized stratigraphic cross section of the Midland Basin-Eastern Shelf transition. The star marks the approximate location of Happy Spraberry Field (after Layman, 2002).

changes that occurred during sedimentation on the platform and in the basin (Handford, 1981).

Originally, the reservoir at Happy Spraberry Field was interpreted to be part of the Spraberry Formation (figure 5) but recently seismic correlations confirmed that it was part of the Clear Fork Formation (Layman, 2002). Oolitic grainstones, packstones, and skeletal bindstones that exhibit some mound segments in growth position also confirm that the environment of deposition of Happy Spraberry Field reservoir rocks was tropical, normal marine, and moderately agitated by waves and currents. Traditionally this environment is called a “shallow marine platform” setting. Because the location of Happy Spraberry Field does not coincide with the Strawn reef trend along the Eastern Shelf, but rather to the sloping surface of the distally-steepened ramp, previous workers had interpreted Happy Spraberry reservoir rocks as re-sedimented debrites and grainflow deposits. This study, following Hammel (1996) identified biogenic structures in growth position and crossbedded grainstones in normal attitude suggesting that the Happy Spraberry reservoir depositional succession is in its original orientation.

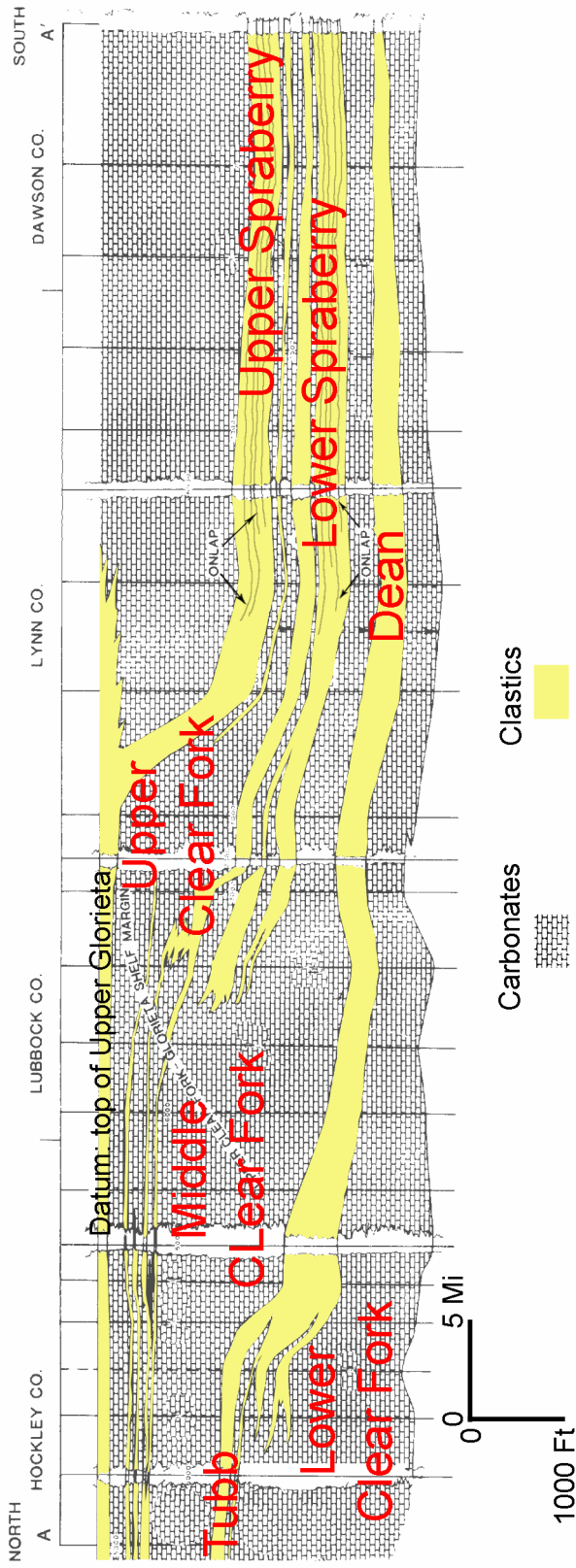


Figure 5. Shelf to basin stratigraphic correlation. Diagrammatic cross-section showing the stratigraphic position of the Lower Clear Fork Formation in the Happy Spraberry Field area (modified after Handford 1981).

METHODS

Happy Spraberry Field has been of special interest at Texas A&M University because an exceptional amount of data has been available for study. Several theses have already been completed on this field (see for example Hammel 1996 or Laymann, 2002), but none have answered fundamental questions about the influence of diagenesis on reservoir quality.

Previous work

Hammel (1996) developed a reservoir-quality classification based on combined values of porosity and permeability from whole core analyses. He compared his quality ranked intervals with petrographic descriptions of thin sections in order to find a relationship between petrographic characteristics and reservoir quality. Finally, he generated “slice maps” (maps of successive 10-foot intervals) of the reservoir to portray three-dimensional relationships between depositional facies and poroperm-based reservoir quality. Although the stratigraphic setting, depositional environment, and general architecture of the reservoir body are known (Hammel 1996, Ahr and Hammel 1999), controls on variations in reservoir quality within the field remained poorly understood, at least in part because previous petrographic studies did not focus enough on diagenetic alteration of depositional attributes.

Available data

Fourteen of the fifteen wells drilled in the John F. Lott lease were cored and in most cases, whole core analyses were done on these cores. Five of the cores were carefully examined by Hammel (1996) and sampled to obtain 125 thin sections for petrographic study. The thin sections were stained with Alizarin Red S to detect dolomite. Only thin sections from the principal reservoir facies were examined for this

study. After initial study, the wells for this study were chosen depending on the following criteria: (1) wells that penetrated mainly carbonates, (2) wells that were cored in the carbonate intervals, (3) cores that underwent laboratory measurements and (4) cores from which thin sections had already been cut. This resulted in the selection of the three wells summarized in Table 1.

Table 1. Data available in the studied wells.

Well	Cored depth		Whole core analysis		Thin sections
	from [ft]	to [ft]	from [ft]	to [ft]	
19-4	4910	4951	4910	4950 ft	21
	4956	5016	4956	4963	
19-7	4963	5053	4963	4999	21
			5011	5013	
19-8	4916	4928	4916	4928	15
	4976	5036	4976	4998	

The reservoir facies are represented in all of the selected wells. Borehole logs were available for each of the wells. In the laboratory, whole core samples were measured for (1) maximum horizontal permeability and horizontal permeability at 90° from the previous direction, (2) vertical permeability, (3) density, (4) porosity, (5) water saturation and (6) oil saturation. Cores were slabbed and half of each core was kept for description and further sampling. The other half was cut in pieces about one foot in length. Whole core analyses were performed on these slabs rather than on standard 1-inch plugs; therefore the values in the core analyses represent average values on one foot intervals. Fluid losses from handling the cores and from environmental differences between surface and reservoir conditions are important. For example, total saturation values from the core analyses ranged from 40 to 80%, far less than the expected 100%.

Nature of this study

Interpreting diagenetic influence on reservoir quality depends on petrologic and petrographic observations. Although petrographic descriptions of Happy Spraberry Field thin sections are reported in Hammel (1996), detailed interpretations of diagenetic variations have not been closely related to variations in reservoir quality. This study focuses on those relationships. Cores were described and compared with existing descriptions to ensure consistency. Thin sections were examined in detail under the petrographic microscope to identify depositional and diagenetic characteristics. Ultimately the petrographic characteristics of good, intermediate, and poor reservoir zones were identified to generate a geological model that explains the origin and degree of connectivity of reservoir zone types.

Depositional and diagenetic textures, mineralogical composition, and fabrics were distinguished and classified separately for each thin section. Subsequently, formative process such as ordinary detrital or biogenic deposition, diagenetic cementation, replacement, recrystallization, compaction, and dissolution were identified in order to establish relationships between current and original rock properties for each reservoir quality category. Care was taken to track relationships between types of diagenetic events and the relative timing of each event during burial history.

Although Hammel (1996) attempted to build a porosity-permeability model for the Happy Spraberry Field reservoir, the results of his work did not clearly identify cause-effect relationships between diagenesis and pore characteristics. This study focuses on how porosity relates with permeability in the reservoir in order to identify patterns of pore types and diagenetic processes/events.

LITHOFACIES AND DEPOSITIONAL ENVIRONMENT

Lithofacies were identified by describing rock composition, texture and sedimentary structures in cores and thin sections. Most of this work had already been done by Hammel (1996); therefore, the main task to be done in this study was to evaluate Hammel's work and confirm his identifications and descriptions before doing more specific evaluations of the effect of diagenesis on reservoir quality.

Lithofacies

Six main lithofacies were identified. They are described in the following paragraphs. Complete description of the cores is available in Hammel (1996).

Oolitic skeletal packstones and grainstones

Oolitic-skeletal packstones and grainstones are the main reservoir rock at Happy Spraberry Field (figure 6). They are present in all producing wells and range from 15 to 70 feet thick. In cores, they typically are pale to light gray but darker brown where oil stained. Most of the ooids and skeletal fragments are partly or completely dissolved and as a result, moldic porosity is important. This lithofacies, particularly in the grainstones, underwent the greatest dissolution of all lithofacies in this reservoir. The average grain size in oolitic grainstones is 0.3 mm and is slightly less in packstones. The other grains consist of skeletal fragments of crinoids, bryozoans, brachiopods, mollusks, ostracods and foraminifera. Ooids comprise more than 75% of all grains in the grainstones and are the dominant constituent of packstones as well. In packstones, ooids are spherical and well rounded; consequently they readily reveal any deformation and fractures. Faint crossbedding is rarely visible.

Lime mud is absent in grainstones but is found as a matrix comprising 5% of the packstones. This matrix consists of both siliciclastic silt and lime mud.

Alternations of oolitic grainstone and packstone beds are present on the upper part of the limestone sequence. These beds lie on the top of the paleostructure and are flanked by rudstones and siltstones. Oolitic packstones can be found interfingering with the rudstones. In this case, if the ooid content is less than 50%, the facies are considered as rudstones. Oolitic grainstones and oolitic packstones were to be deposited in a moderately agitated, shallow marine, tropical environment. Ooids are absent in modern temperate environments and are generally interpreted to be indicators of tropical climate in ancient settings as well.



Figure 6. Core photo of oolitic grainstone at 4933 feet, well Lott 19-4. Note well developed skeletal-moldic porosity.

An uncommon feature not described in previous studies on Happy Spraberry Field, is that ooids are bi-mineralic. Most modern marine ooids are composed of aragonite and have a tangential fabric. High-Mg calcite ooids have not been observed to form in modern seas. Mixed calcitic-aragonitic ooids are presently forming in the hyper-hypo saline Baffin Bay, Texas and are common in the rock record. They show radial cortical layers of high-Mg calcite and tangential and micritic coatings of aragonite (Land et al., 1979). Although the factors that influence ooid mineralogy in Baffin Bay are unknown, Tucker (1984) suggests that these bi-mineralic ooids reflected geochemical changes within this partially isolated bay. Precipitation conditions would change dramatically as a result of storms or rapid continental run-off. Chow and James (1987) examined bi-mineralic ooids from the Middle and Upper Cambrian platform carbonates in western Newfoundland, Canada. They suspect more widespread organic and chemical control. Heydari et al. (1993) observed two-phase ooids in the Pitkin Formation, North-Central Kansas. They suggested that bi-mineralic ooids were precipitated at the transition between two paleoenvironments, one precipitating aragonitic ooids and the other one precipitating calcitic ooids. Pratt (2001) suspects cyclic variations in the maximum depth range of the aragonite compensation depth in warm water based on his study of the Helena Formation, western North America.

Most of the ooids in the Happy Spraberry Field are partially or completely dissolved. Some ooids show selective dissolution that left only a ring-shaped structure as a partial grain mold (figure 7). High-Mg calcite segments of the ooids appear to be removed by dissolution, whereas the aragonite that stabilized to calcite prior to dissolution remains. This selective dissolution is interpreted as evidence that the ooids are bi-mineralic. The rare occurrence of two ring-shape concentric structures in the same mold suggests that environments favorable to dissolution, stabilization, and precipitation were cyclical.

Better reservoir rock properties are found in the oolitic packstones, which exhibit higher porosity and permeability than the oolitic grainstones. This may seem to counter-intuitive and will be discussed below.

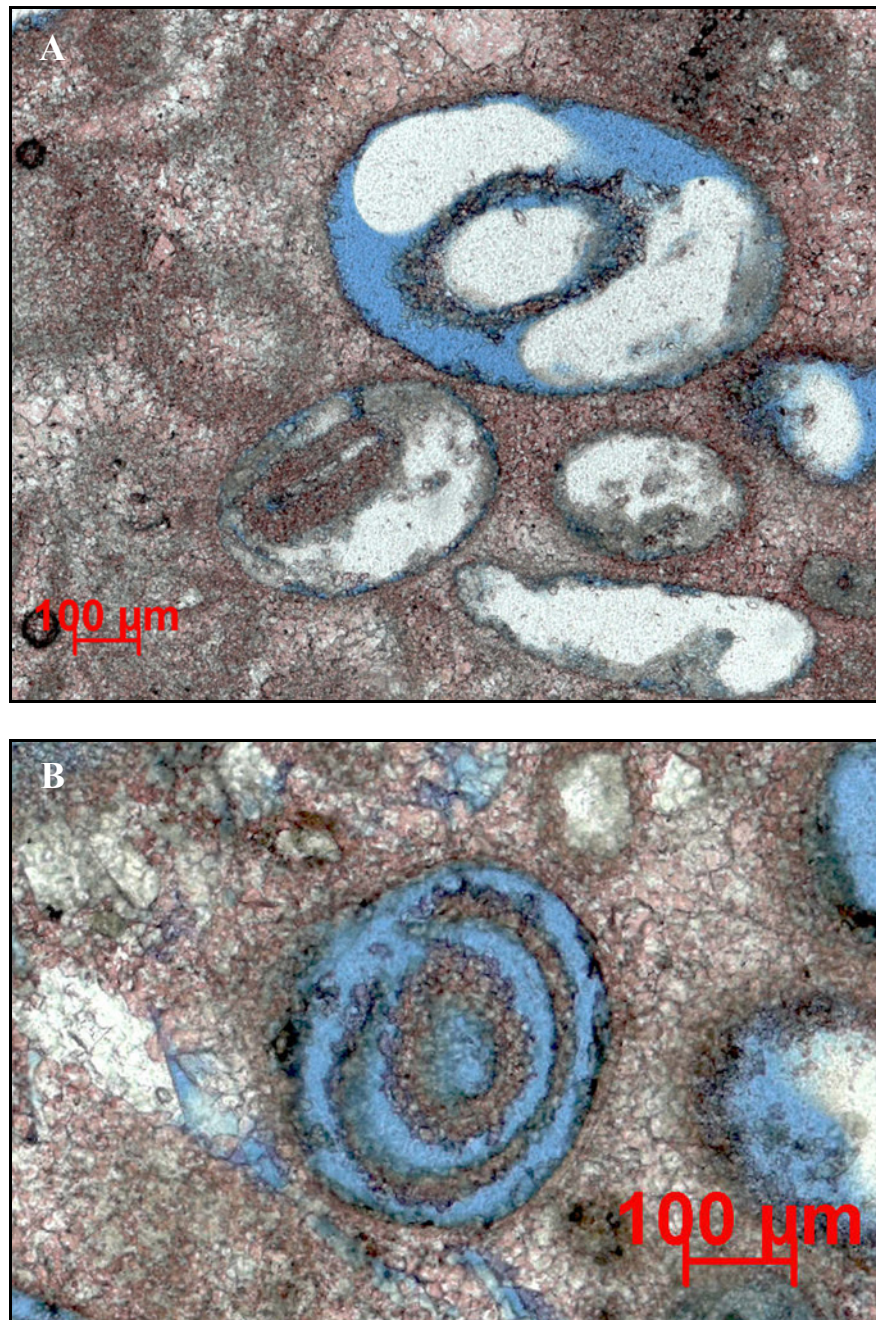


Figure 7. Ring shaped structures left by selective dissolution within ooids. A) Single ring shaped structure from a sample at 4919.3 feet, well Lott 19-4. B) Double ring shaped structure from a sample at 4957.5 feet, well Lott 19-4.

Floatstones and Rudstones

Hammel's subsurface correlations indicate that floatstones and rudstones are time-equivalent to the oolites (figure 8). Rudstones have grains that range in size up to 10 cm and are mainly clast-supported rocks. Floatstones have much more lime-mud matrix and smaller clasts (maximum 5cm). Clasts consist in oolitic facies and skeletal fragment. Skeletal fragments are larger and better preserved in the rudstones, probably because they underwent less transport. Rudstones are adjacent to the oolitic grainstones; floatstones are farther away. Shale laminations of about 1 mm thick are occasionally observed in rudstones. Oolites may be interbedded with rudstones, but the proportion of ooids is always less than 50% of total grain content. Siliciclastics may be common in the rudstones and floatstones. Pores in the rudstones are usually large vugs that, depending on connectivity in the vuggy pores, can be medium-quality reservoir rocks. Floatstones are so muddy that they exhibit very little porosity. Instead, they make good seals. Both floatstones and rudstones are stylolitized, although no study has been done to assess the influence of stylolites on reservoir connectivity at Happy Spraberry Field.

Bindstones

The bindstone facies were first observed by Hammel (1996) in wells 19-4 and 19-7, adjacent to floatstone and rudstone facies. Organisms are found grouped together in growth position forming bindstones rich in bryozoans, mollusks, crinoids and *Tubiphytes*. Nowhere in the cores available could these bindstones be found as clasts; they are interpreted as reef material or *in situ* biogenic buildup (figure 9). *Tubiphyte* is an encrusting alga that commonly develops in association with *Archeolithoporella* and builds skeletal biotic communities during the Permian (Sano et al., 1990). It is commonly observed in several places in the world among which southern Alps, southern Tunisia, central Texas, west Texas and New Mexico.

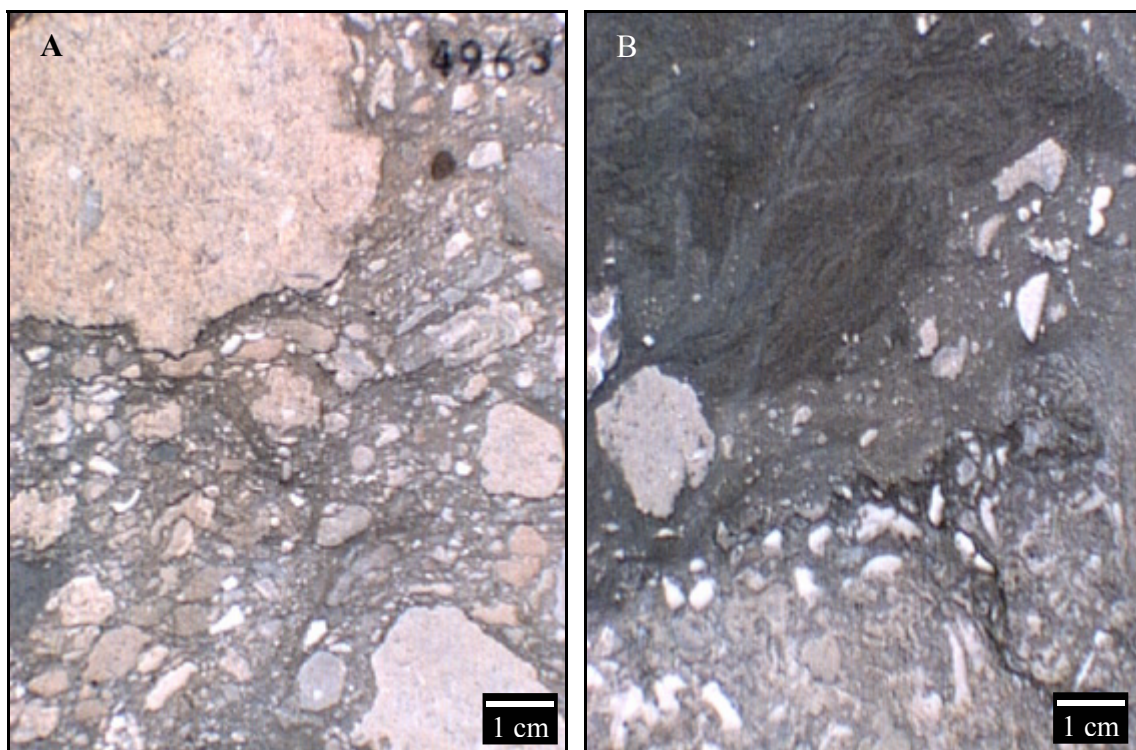


Figure 8. Core photo of rudstones and floatstones. A) Rudstone at 4963 feet, well Lott 19-4. B) Floatstone at 4981 feet, well Lott 19-4.



Figure 9. Core photo of *Tubiphytes* bindstones. Core sample is from 4971 feet, well Lott 19-4. The bindstone, or reefy material is located in the right portion of the photo adjacent to floatstone clasts.

Siliciclastics

Siliciclastics are either shaly siltstones or very fine-grain sandstones (figure 10). They are light gray to medium brown in color. Quartz silt is, by far, the main element of these rock types. The same skeletal fragments observed in the other facies are present here but in smaller proportions. The rest of the matrix consists of clays and lime mud. Laminations with shales, ripples and soft sediment deformation were observed.



Figure 10. Core photo of siliciclastics. Core sample is from 4975 feet, well Lott 19-4. Note wavy ripples (black) near center of photo.

These facies are non-reservoir facies because the abundance of matrix and to an extent, carbonate cementation has prevented the development of permeability. High shale-content or extensively cemented silts are a seal for the field.

Depositional environment

Depositional environments were identified from core description and thin-section petrography. A depositional model was derived using previous work done by Hammel (1996).

Siltstones, fine-grain sandstones and shales are found at the stratigraphic base of the field. These inferred slope sediments provided the paleotopography for the later deposition of shallow-water carbonate buildups and grainstone shoals. Fine grain size, high clay content and planar bedding suggest that these siliciclastics were deposited in a low energy environment and at water depths greater than 50 meters.

Bindstones developed on paleotopographic highs to localized skeletal banks that mainly grew by aggradation. These framework building organisms required a tropical, shallow water environment with warm water within the euphotic zone. Adjacent to topographic highs are rudstones and floatstones formed from eroded material from the buildups by waves, storms and normal breakdown.

Packstones and grainstones are located on top of the buildups where they interfinger with the skeletal bank deposits. The presence of well sorted coated grains and skeletal fragments suggests agitated shallow water within fair-weather wave base.

Field geometry and well location

Field geometry is difficult to establish without seismic data. The field consists roughly of two pods, one in the South and one in the North (figure 11). These two pods rely on local tops of the paleotopography of the late Pennsylvanian siliciclastics. On these tops, reef bindstones developed surrounded and overlain by rudstones. The

floatstones are found further away. On top and interfingering with the rudstones, are the oolitic-skeletal packstones overlain by the oolitic grainstones.

In the south part of the field, well Lott 19-7 carbonates are mainly bindstones (30 feet) and rudstones (30 feet) that interfinger with some packstones (10 feet). In the northern part of the field, wells Lott 19-4 and Lott 19-8 are located on a pod composed of a thin bindstone layer overlain by rudstones and thick oolites made of both oolitic-skeletal packstones and oolitic grainstones. Well Lott 19-4 shows fewer rudstones but a thick and large shoal mound in which intervals of purely oolitic grainstones with no mud can be found among packstones. On the edge of this pod, well Lott 19-8 shows more mixed facies. It exhibits rudstones with high ooid content and oolitic packstones that are mixed with many skeletal fragments. The continuity of the shoal mound from well 19-4 to well 19-8 is certain. Laymann (2002) suggests continuity between the northern mound and the southern one, but there is no conclusive evidence of this.

Laboratory measurements were only performed in producing intervals. In well Lott 19-7, porosity and permeability values are available in the bindstone, rudstone and oolitic packstone facies. Rudstones and oolitic packstones undergone measurements in well Lott 19-8. In well Lott 19-4, the producing interval is composed of oolitic grainstones with some oolitic packstones and very few rudstones.

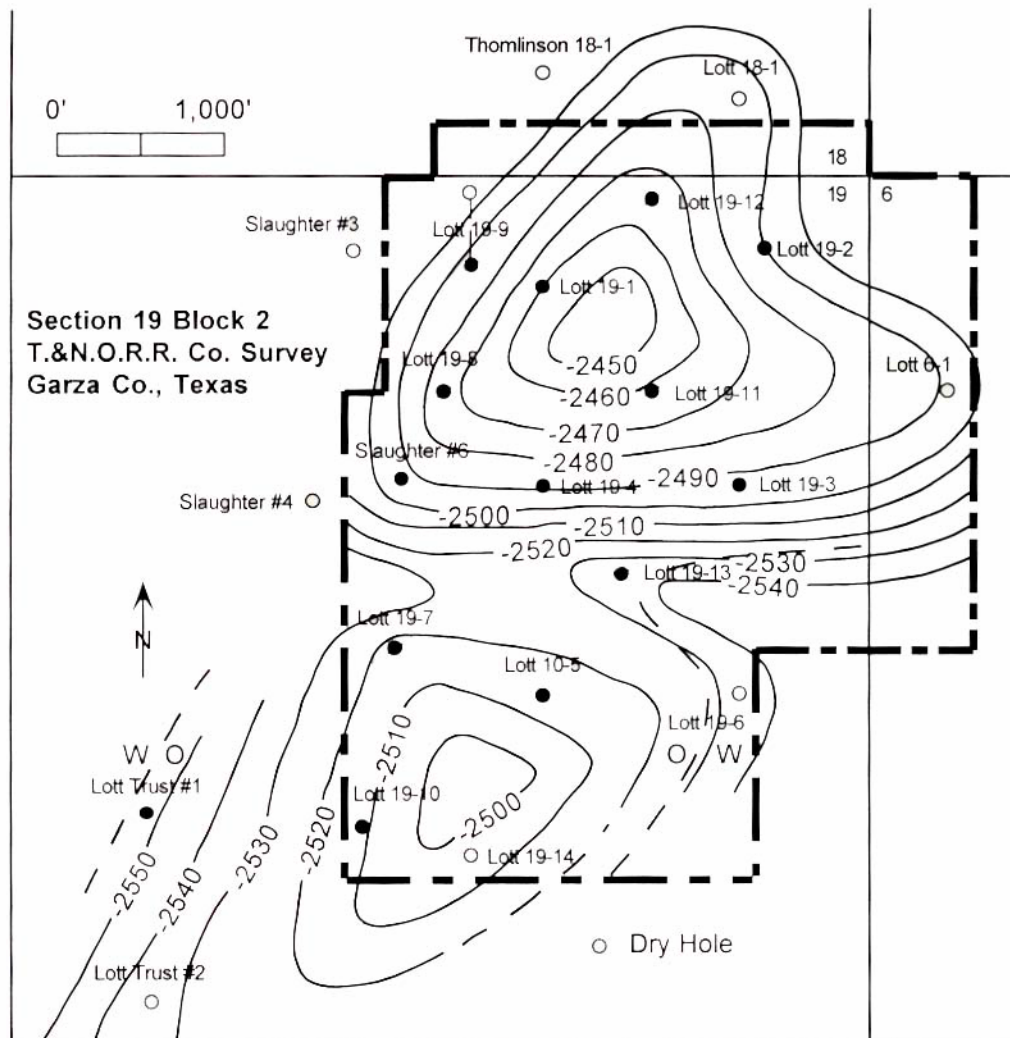


Figure 11. Structure map on top of the Happy Field carbonates.

DIAGENESIS

Interpretation of diagenetic changes and sequences of diagenetic events is based on thin section petrographic study. Diagenetic features were described and located and timing of diagenetic events in chronostratigraphic sequence was done by studying cross-cutting relationship between different diagenetic features.

Description of the diagenetic features

The diagenetic history of the Happy Spraberry Field is complex and occurred in different environments. The processes described below happened approximately in chronological order. Only one paragraph is dedicated to dissolution but it occurred in several phases. Almost all grains and cements exhibit dissolution features.

Shallow marine diagenesis

Micritic envelopes

In the oolitic grainstones and packstones, some of the ooids and skeletal fragments show a micritic envelope (figure 12), a thin and black coating around the grains. In some cases the grain has been dissolved and the micritic envelope is still visible. It is not present on all grains and its recognition can be difficult where there is isopachous cement. The micritic envelope is also observed around skeletal fragments in rudstones and floatstones.

Skeletal debris and ooids lying on the sea floor are attacked by boring organisms such as algae, cyanobacteria and fungi. When left by the organism, these small bores (few microns to tens of microns) are filled with micritic cement and eventually form an envelope (Tucker and Wright, 1990).

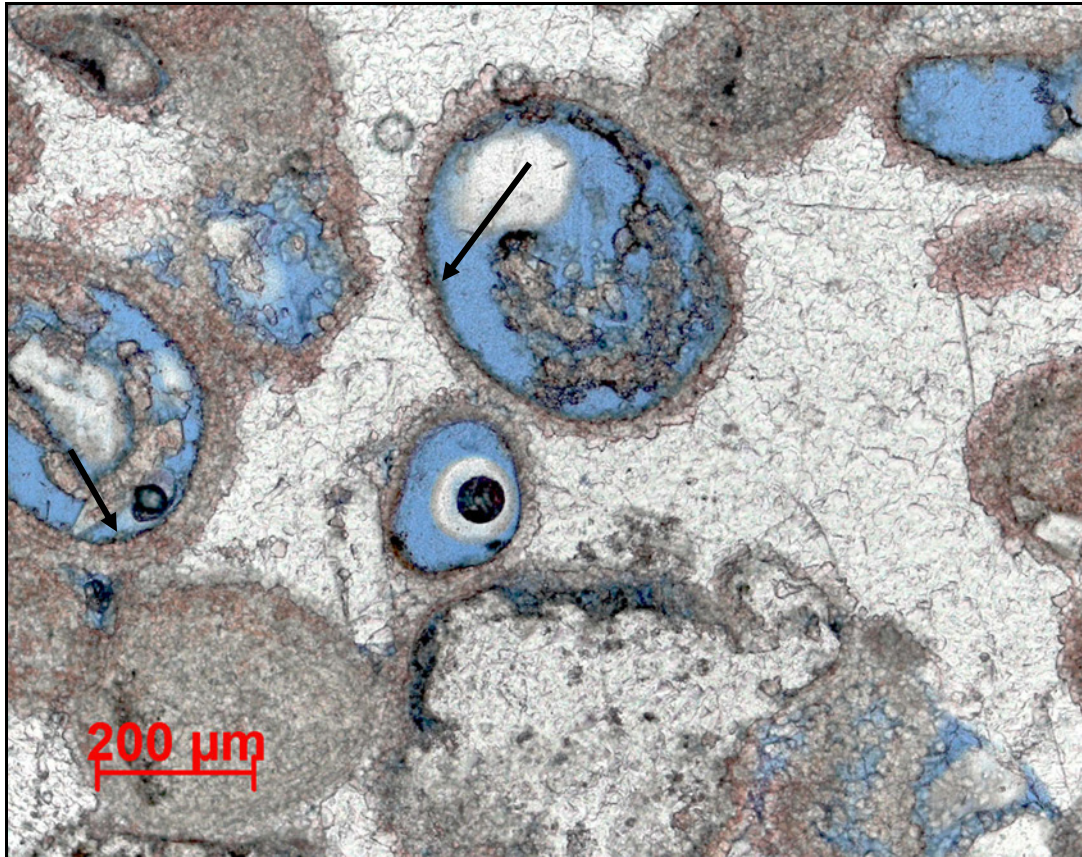


Figure 12. Thin section photograph showing isopachous circumgranular calcite cement colored by Alizarin Red S stain. Stained calcite is surrounded by poikilotopic anhydrite. Note the relict micrite rims just beneath the rim cement (arrows). Photo is from a sample at 4930.1 feet, well Lott 19-4.

Isopachous cement

Circumgranular isopachous calcite cement with bladed rind is always found in the oolitic grainstones either directly on the ooid or on its micritic envelope (figure 12). This cement often shows dissolution either on the grain side or on the outer side. This isopachous cement is less common in oolitic packstones and is rare in rudstone facies, and if present, dissolution was significant. Rudstone and bindstone facies form in low energy environments where wave energy is not sufficient to make water pass through the sediment and precipitate its dissolved elements. Oolitic grainstone form in environments higher in energy and there is more cementation through seawater pumping (Tucker and Wright, 1990).

Other early processes

In the shallow marine environment, two of the very first diagenetic events are (1) the stabilization of skeletal fragments from aragonite or high-Mg calcite to low-Mg calcite and (2) the recrystallization of lime mud to neomorphic microspar (Tucker and Wright, 1990).

Shallow burial diagenesis

Calcite cement I

In oolitic grainstones, drusy calcite cement precipitated directly on the isopachous cement (figure 13). This cement either completely filled intergranular porosity or left some remnant porosity. In case of moldic-enhanced porosity, it can show some dissolution on the ooid side. This cement is also common in packstones and is rarely seen in rudstones. Spatial variability of this cement in the oolitic grainstones is strong and important. In some samples it extensively filled the depositional pore system; in others it is rarely observed.

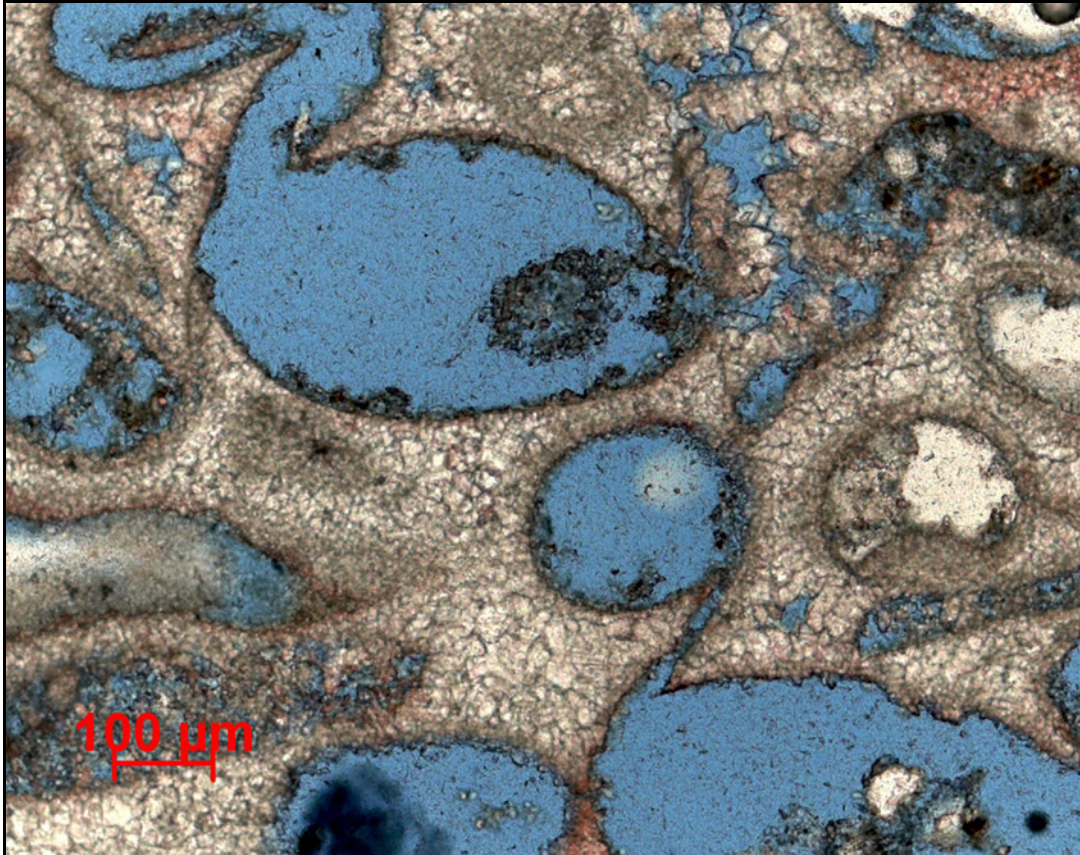


Figure 13. Circumgranular isopachous cement and calcite cement I broken by compaction, from a sample at 4919.3 feet, well Lott 19-4. Drusy calcite cement I is well seen in intergranular porosity.

Dissolution

Dissolution produced most of the effective porosity. Moldic porosity is usually more pronounced than intergranular porosity. It occurred in several phases and all facies and cements were affected. Most of the ooids in oolitic grainstones and packstones were affected by an early and selective dissolution phase. This dissolution can be incomplete, complete or enhanced. Ooid dissolution phase was the most intense of all but even though, its effects throughout the oolitic grainstones are variable. In the oolitic packstones, ooids are less affected than in the oolitic grainstones and some muddy samples were well protected.

Ooids are partly or completely dissolved in the other facies. Dissolution of skeletal fragments produced less systematic vuggy porosity.

Compaction

The effect of compaction on oolitic grainstones and packstones is variable. In oolitic grainstones compaction affected molds generated during the previous dissolution phase. It can break isopachous cement and calcite cement I connecting adjacent molds. Where calcite cement I is absent or sparse, compaction distorted mold structure connecting adjacent molds. Where dissolution of the ooids was less intense or where calcite cement I more completely filled intergranular pore space, well rounded ooid molds are preserved (figure 14). In oolitic packstones, effect of compaction is less obvious and most oolitic molds are well rounded.

In rudstones, effects of compaction are much less evident because the original structure is not easy to recognize. Many skeletal fragments are undeformed. On cores, some stylolites are observed.

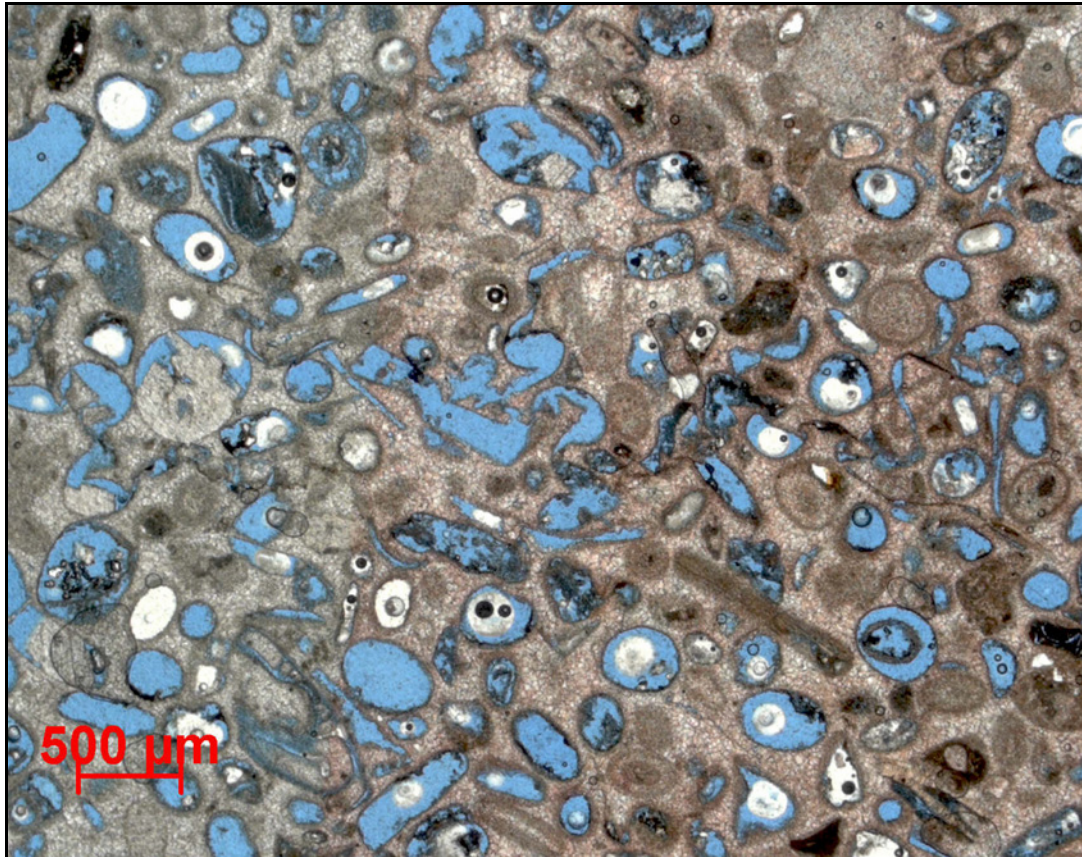


Figure 14. Effect of compaction from a sample at 4926.9 feet, well Lott 19-4. In the middle of the photograph, connectivity between molds has been enhanced by compaction where cements were less widespread.

Deep burial diagenesis

Calcite cement II

Another phase of calcite cement, calcite cement II, is coarser, blocky and clearly post-compaction (figure 15). In oolitic grainstones and packstones, this cement is common and can be found in the remnant extra-granular porosity or even ooid molds. In rudstones and bindstones, calcite cement II is observed in large vugs. Interfaces between calcite cement I and calcite cement II shows no dissolution features. Crystal size is typically in the order of 100 μm .

Calcite cement III

Calcite cement III represents a small volume in the overall rock. It is very coarse (crystals are commonly around 500 μm in size and even larger in some samples) and can completely fill vuggy porosity found in rudstones and bindstones (figure 16). It was rarely found in the oolitic grainstones and packstones.

Anhydrite

Anhydrite occurs as a poikilotopic cement that extensively fills the inter-granular porosity and some molds (figure 17) in the oolitic grainstones. Its repartition is variable and when present it is an important porosity reducer. Anhydrite has been affected by late stage dissolution. Where dissolution has been intense, molds filled with anhydrite can have parallel extinction even where no continuity of the anhydrite is observed in the plane of the thin section. Anhydrite is abundant in oolitic grainstones of well Lott 19-4, and is rarer in facies of wells Lott 19-7 and Lott 19-8. Anhydrite was clearly precipitated after the beginning of compaction but before complete fracturing of dissolved ooid pores. Origin of anhydrite is not known. Above Clear Fork Formation, the San Andres formation (Lower Guadalupian) shows dolomite plugged with anhydrite. The latter comes from the overlaying Yates Formation (Upper Guadalupian) which is a mix of

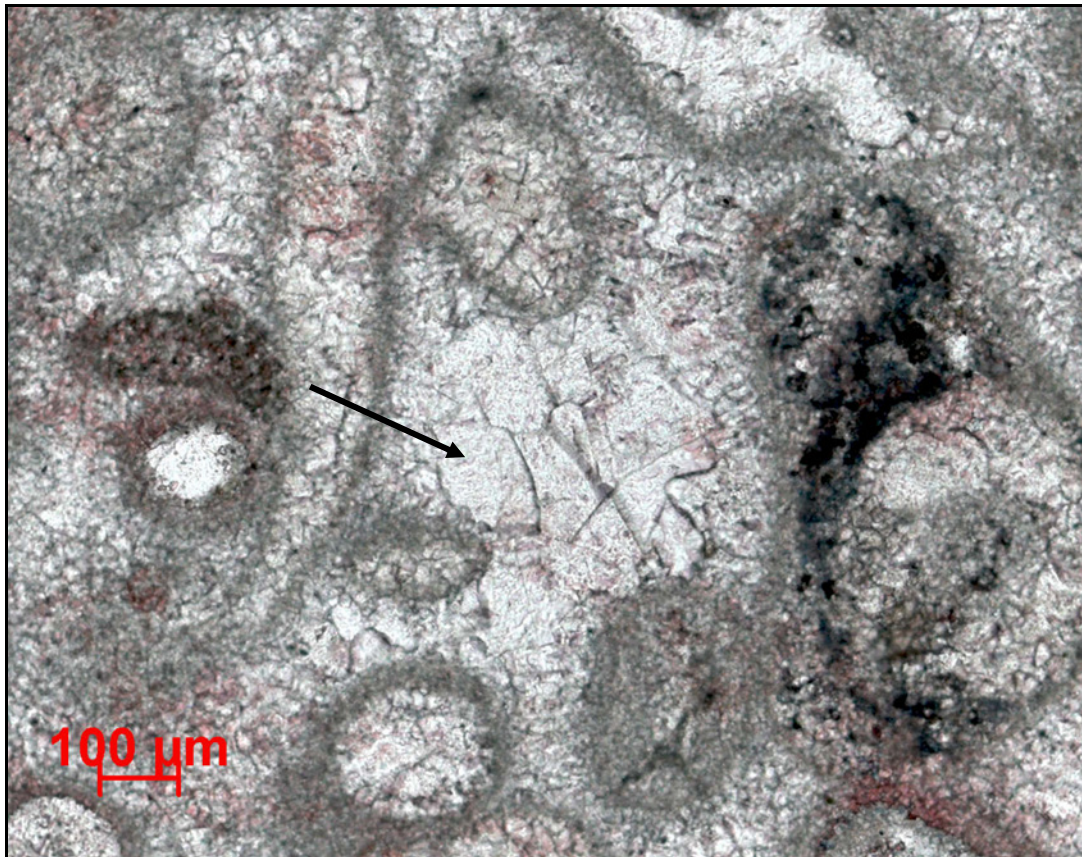


Figure 15. Calcite cement II from a sample at 4919.3 feet, well Lott 19-4. Arrow shows calcite cement II crystals filling remnant intergranular porosity.

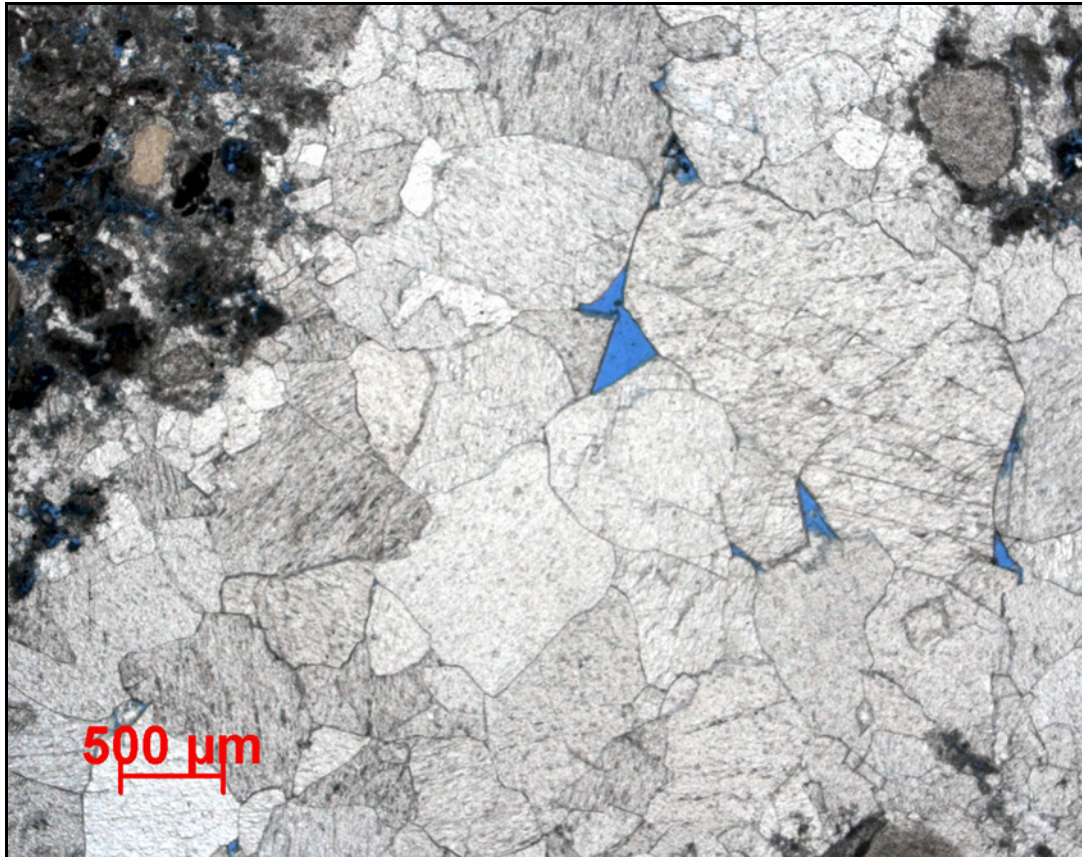


Figure 16. Calcite cement III from a sample at 4981.5 feet, well Lott 19-8. Calcite cement III extensively fills vuggy porosity in rudstones.

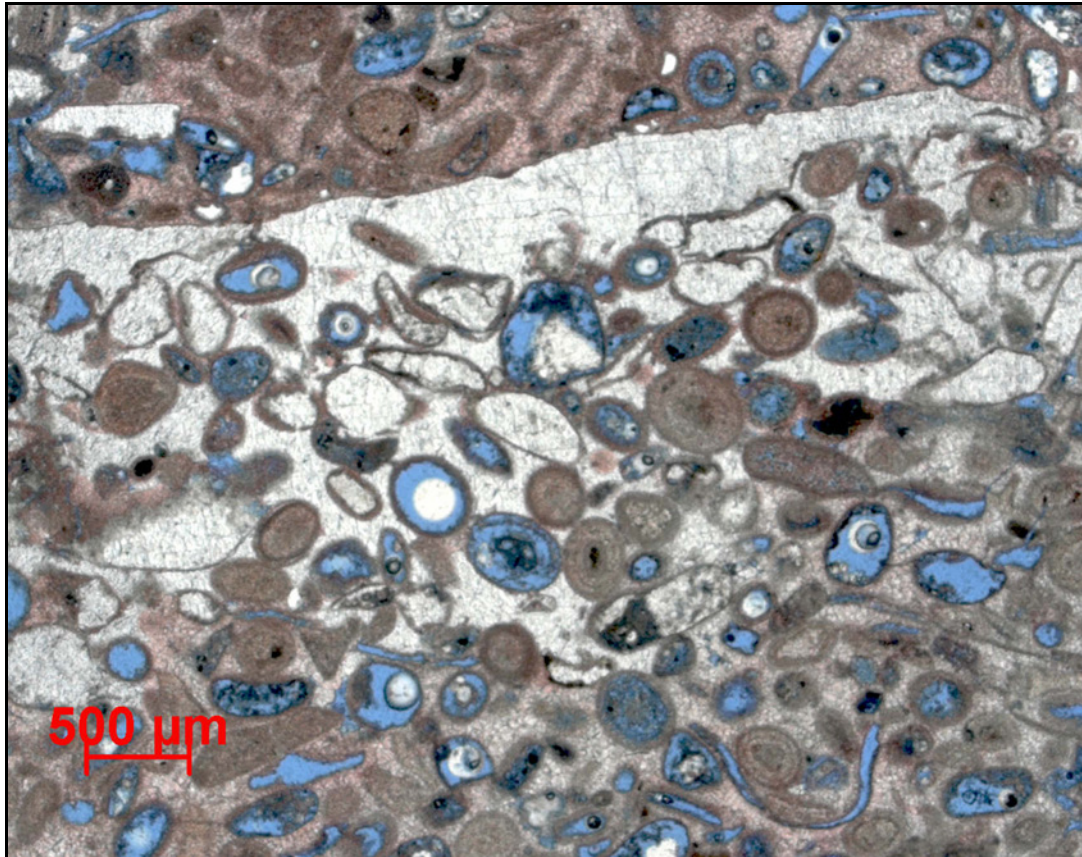


Figure 17. Anhydrite from a sample at 4933.1 feet, well Lott 19-4. Poikilotopic anhydrite fills extensive intergranular porosity and part of the moldic porosity. Anhydrite precipitation started after the beginning of mechanical compaction.

clastics and evaporites (Ward et al, 1986). These formations are possible sources of anhydrite for the Lower Clear Fork formation.

Saddle dolomite

Saddle dolomite can be identified by its undulose extinction, curved boundaries and a cloudy appearance (figure 18). All occurrences of saddle dolomite in this study showed signs of dissolution, mainly corroded crystal boundaries. The rhombs are among the biggest crystals (in the order of 500 μm); they usually fill cavities such as dissolved ooids or vugs. Saddle dolomite is found mainly in rudstones and bindstones and is less common in oolitic packstones where the skeletal-fragment content is high. Saddle dolomite was rarely observed where there is anhydrite cement. It usually represents no more than 5% of the thin section, except in well Lott 19-7 where it is abundant.

Pyrite

Few small clusters of pyrite were observed sporadically in the facies.

Chalcedony

Chalcedony replaces calcite shells and cements in all facies including sandstones (figure 19). It always shows a spherulitic arrangement. Chalcedony is unimportant in volume.

Effect of diagenesis on porosity

The succession (1) circumgranular isopachous cement, (2) calcite cement I, (3) dissolution of ooids, (4) compaction, (5) calcite cement II, is clearly identified in the oolitic grainstones and packstones by cross-cutting relationships. Precipitation of anhydrite, saddle dolomite and chalcedony happened after that, in unclear chronological order. Diagenetic events are summarized in figure 20.

Diagenesis has been selective. Among all grains, ooids show the most intense dissolution. A large majority of them are dissolved in the oolitic-skeletal grainstones and

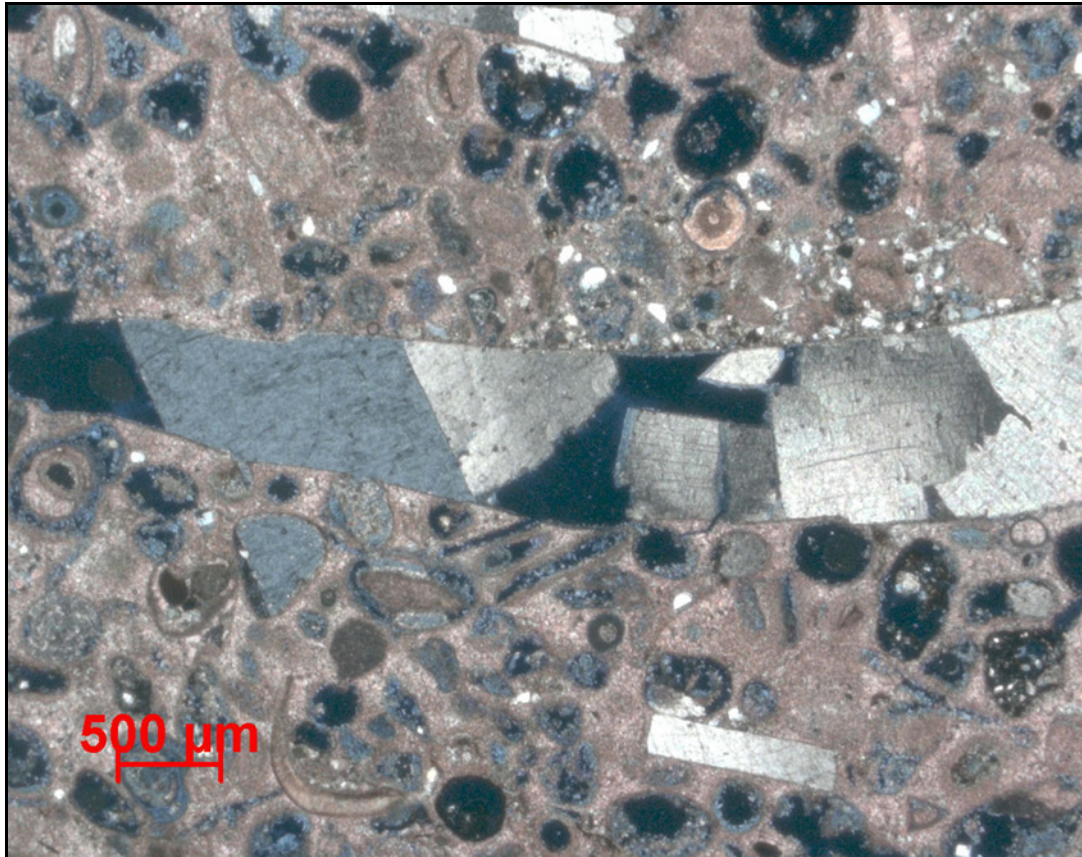


Figure 18. Saddle dolomite from a sample at 4960.6 feet, well Lott 19-4. The photograph is taken using the crossed Nicols. Saddle dolomite is clearly identified in the large skeletal mold by undulose extinction, cloudy appearance and curved crystal boundaries. It also shows dissolution. Gray crystal that shows a single extinction on the left of the mold is anhydrite.

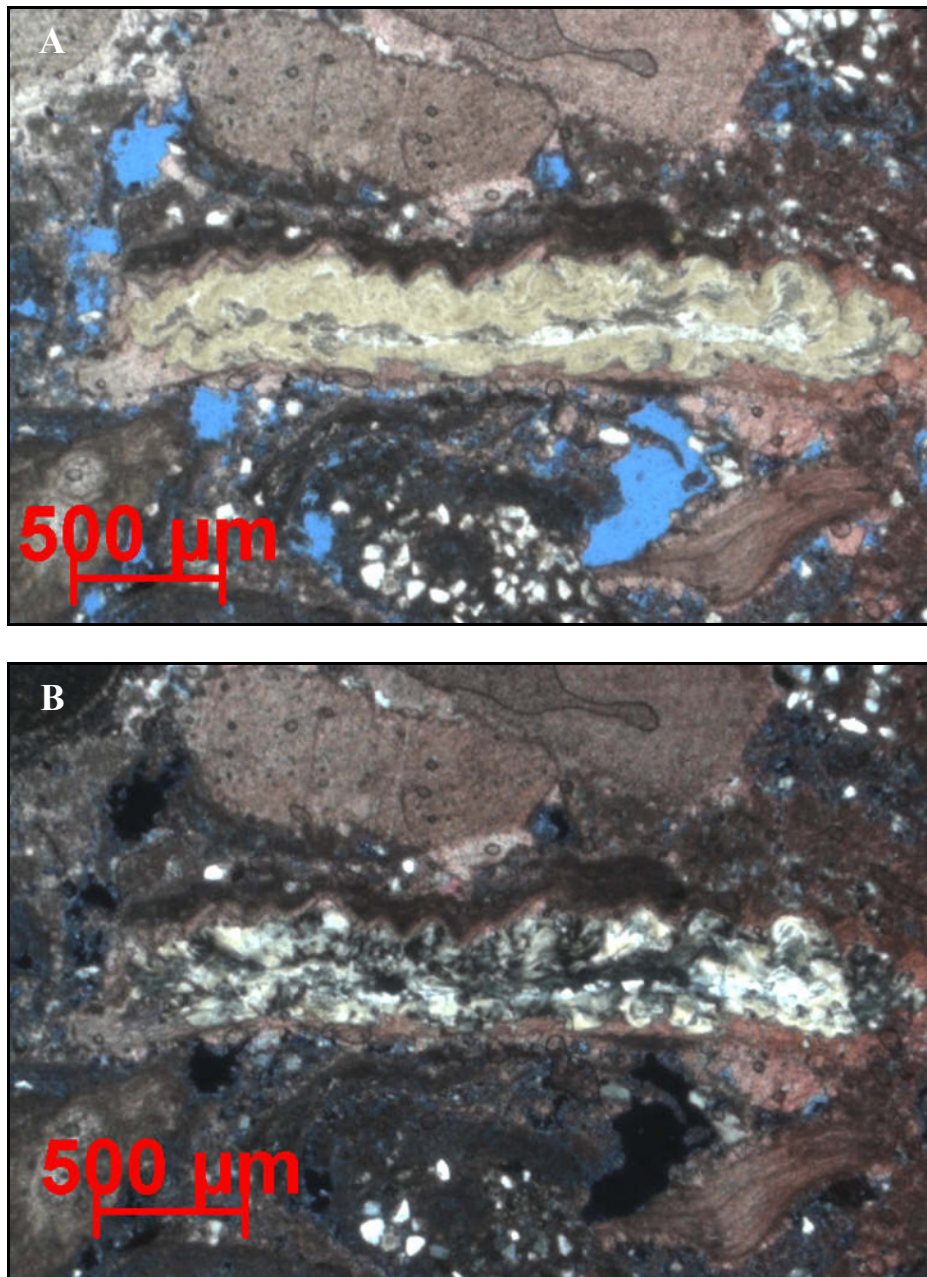


Figure 19. Chalcedony replacement from a sample at 4982.2 feet, well Lott 19-8. A) Plain light photograph that shows chalcedony replacement in a skeletal fragment. B) Same view with the cross Nichols. Note that the chalcedony exhibits spherulitic microstructure.

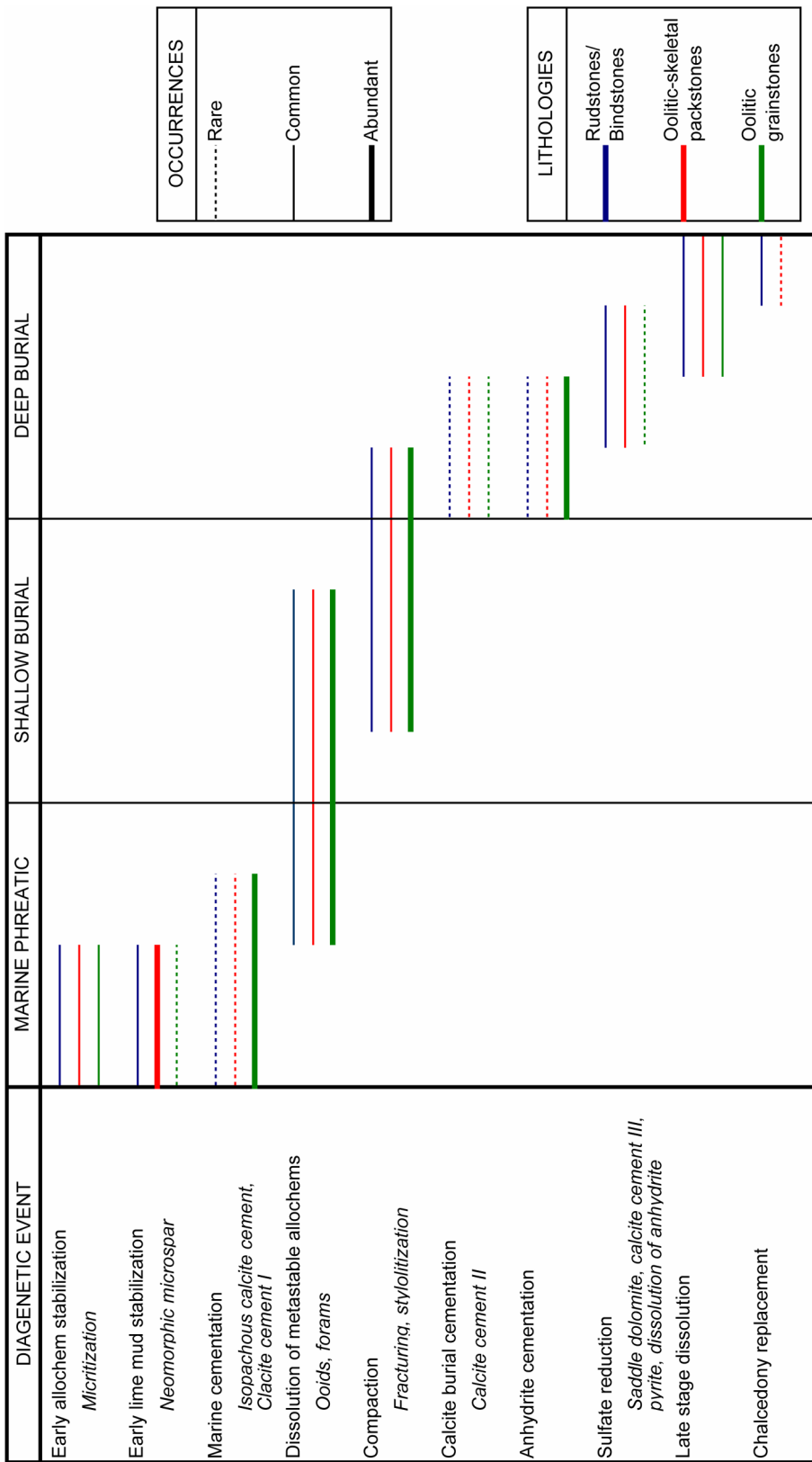


Figure 20. Diagrammatic summary of diagenetic environments at Happy Spraberry Field.

packstones. Ooids are also well dissolved in rudstones. The skeletal fragments were also affected by dissolution, but not as much as the ooids.

Diagenesis has been intense. Dissolution, especially of ooids, was important. Moldic porosity overprints depositional porosity in packstones and grainstones.

Diagenesis has been variable. Grainstones underwent the most intense diagenesis. Packstones also were strongly affected, but not as much as grainstones. Rudstones and bindstones, because of their poor ooid content, underwent less dissolution. Diagenesis has also been variable within grainstones. In these facies, the relationship between (1) calcite cement I, (2) dissolution and (3) compaction controls reservoir quality in association with (4) anhydrite pore filling. Calcite cement I occurrence is variable with zones of extensive filling of intergranular porosity and zones of little cementation. Because of dissolution, compaction fractured the molds where calcite cement I was not extensive enough to hold the structure. This breakage reduced porosity and increased connectivity between the molds. Where calcite cement I is widespread, molds are still well-rounded and unfractured; they are not connected. After compaction and only in sparse samples, anhydrite filled the intergranular pores and some of the molds. In such cases, little porosity and no connectivity are left. In the packstones, neomorphosed mud prevented any breakage of the molds and connectivity is poor; some fracturing are observed, but never complete collapses of molds.

In rudstones and bindstones, porosity was mainly intergranular (sometimes enhanced by dissolution) between clasts or vugs within the framework. Neomorphosed mud was present and dissolution has been less intense. All cements are found in various proportions. The ooids in rudstones can be completely dissolved, but they show little compaction because they were mechanically protected by the other grains.

Thermosulfate reduction

The origin of saddle dolomite in Happy Spraberry Field samples is not clear. Collins and Smith (1975) suggested that saddle dolomite formation coincided with the

submergence of previously exposed rocks to depths below normal sea level. Asserto and Folk (1980) suggested that saddle dolomite formed after invasion of freshwater into a hypersaline environment. Morrow et al. (1986) suggested that saddle dolomite formed during any of three episodes: (1) freshwater-seawater mixing, (2) thermal convection of brines that dissolved underlying evaporites, and (3) a regional groundwater flow system. According to Machel (1987) there is no conclusive evidence of a low-temperature, low-salinity origin of saddle dolomite.

Machel (2001) discussed bacterial and thermochemical sulfate reduction. Dissolved sulfates and hydrocarbons are thermodynamically unstable at temperatures below 200°C. Sulfate is reduced by hydrocarbons either bacterially (bacterial sulfate reduction) or thermally (thermal sulfate reduction). Both processes form H₂S, coarse calcite cement and, if magnesium is available, saddle dolomite. The reaction rate is controlled by the dissolution rate of anhydrite. The effect on porosity is difficult to predict. Pore space increases where anhydrite is dissolved, but porosity decreases where calcite and saddle dolomite form.

There is no decisive evidence that sulfate reduction occurred in the carbonates of the Happy Spraberry Field. If it did, because of the relatively shallow depth (1,500 metres) and low temperature (110°F) only a bacterially controlled process could have happen (Machel, 2001). Calcite cement III could be the coarse calcite cement which is a by-product of sulfate reduction. The fact that saddle dolomite is mainly observed in rudstones and bindstones where many skeletal fragments could have been dissolved to bring magnesium (stylolites in rudstones and bindstones), is consistent with Machel's theory. Such a phenomenon could explain the presence of pyrite clusters if Fe is available (Machel, 2001). Dissolved anhydrite and oil, which are the reactants, are present in the field. If bacterial sulfate reduction occurred, the reaction would have stopped on its own because the involved bacteria poison their own environment with H₂S in a closed system. In volume, the importance of biodegradation on oil is unknown.

Eggshell diagenesis

The early dissolution and subsequent compaction of the ooids in Happy Spraberry Field can be compared to “eggshell diagenesis” described by Wilkinson and Landing (1978) in the Jurassic Twin Creek Formation of northwestern Wyoming. They observed that the dissolution of the aragonitic nuclei happened early during diagenesis. After loading, the resulting hollow cortical sheaths exhibit distinct fracture shapes in bedding plane and in vertical plane. Aragonite was dissolved and calcitic coatings remained. Nuclei of calcite were not dissolved. Their study shows that micritization of ooid nuclei and cortical coatings by microendolithic organisms both preceded and accompanied ooid formation. Highly micritized ooids with aragonitic nuclei show no fracturing and little deformation due to compaction. This indicates the development of a rigid framework of microcrystalline calcite within and between endolith borings in aragonite grains.

Ooid dissolution in Happy Spraberry Field rarely left an outer hollow sheath. The surrounding cements or mud hold the structure of the mold or are fractured by compaction. Diagenesis in Happy Spraberry Field can not be called “eggshell diagenesis”. The relationship between early micritization and rigidity described by Wilkinson and Landing could explain the preservation of thin ring-shaped structures in Happy Spraberry Field. On figure 7, the remnant cortical layers seem to be fragile. In many cases, the ring-shaped structure is broken within the mold, even if the mold itself is not fractured, but it is common to observe preserved structures. Early micritization could help holding these ring-shaped structures.

Analog studies

On the side of the Midland Basin that faces Happy Spraberry Field is the Southwest Andrews area that comprises Deep Rock, Parker and Andrews oilfields. Stueber et al. (1998) studied the brines origin and migration through their composition in

the series from Devonian to Wolfcampian (Early Permian). Dickson et al. (2001) discussed the diagenesis of carbonates in the Canyon (Missourian), Cisco (Virgilian) and Wolfcamp (Wolfcampian) formations (figure 21). His findings are discussed below.

Description of the cements

During Pennsylvanian and Early Permian time, the structural histories of the eastern and western sides of Midland Basin were very similar and facies in both areas consisted of shelf carbonates. In the Southwest Andrews area, the Canyon, Cisco and Wolfcamp formations have a thickness of about 250 meters and are composed of about 70 sedimentary cycles that formed in response to glacio-eustatic fluctuations of sea level. The middle Wolfcamp Formation, which is the closest in age to the Lower Clear Fork Formation, consists of reef material (Dickson et al., 2001). The formations underwent a four stage cementation. These stages are not regarded as synchronous, but each sample passed through a similar succession of diagenetic environments: (1) stage 1 cements occurs in intergranular pores and is abundant in rocks that were relatively uncompacted. Where mechanical compaction is pronounced, stage 1 cements are fractured, (2) stage 2 cement also formed pre-compaction, overlies stage 1 cement, and occurs in early moldic porosity, (3) stage 3 cement is post-compaction, and (4) stage 4 cement is a late cement that is distributed sporadically throughout the interval. Stage 1 and 2 cements are of marine or meteoric origin; stage 3 and 4 cements are precipitated at depth. Saddle dolomite that postdates stage 3 is present in all the formations.

Even if the interval studied by Dickson et al. (2001) is older than the Lower Clear Fork Formation, and is at greater depth (about 3 kilometers), the description of the four-stage cementation is similar to the four calcite cements observed in the Happy Spraberry Field (circumgranular isopachous cement and calcite cements I, II and III). Isotopes studies performed on Southwest Andrews rocks and $\delta^{13}\text{C}$ values in saddle dolomite are the same as the host limestone. This indicates that dissolving fluids exhibited little cross-formational flow before precipitation; saddle dolomite was

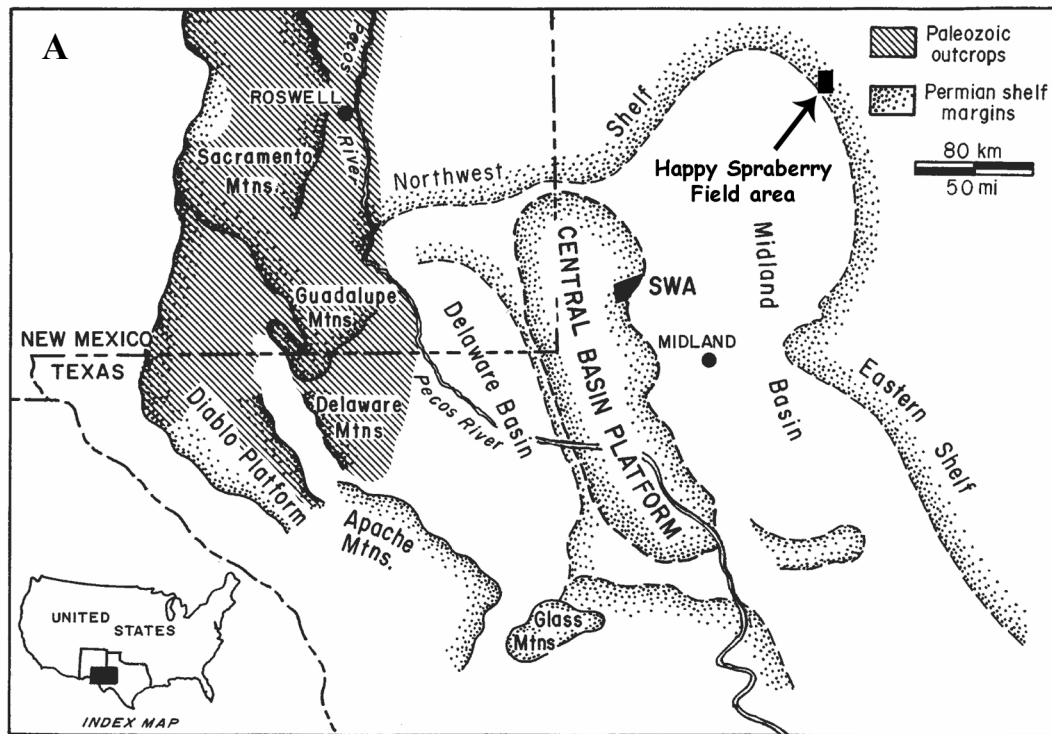


Figure 21. Study of the Southwest Andrews area. A) Map view locating the Southwest Andrews area and the Happy Spraberry Field in the Permian Basin (modified after Stueber et al., 1998). B) Stratigraphy, lithology and hydrogeological units in the Southwest Andrews area. Stratigraphic units from which formation-water samples were produced are shaded (after Stueber et al., 1998).

B

System	Series	Group/Formation	General Lithology	Hydrogeological Unit*	
<i>Tertiary</i>		<i>Ogallala</i>	<i>fluvial and lacustrine clastics</i>	<i>Upper Aquifer System</i>	
<i>Cretaceous</i>		<i>Fredericksburg</i>	<i>limestone sandstone</i>		
		<i>Paluxy</i>			
<i>Triassic</i>		<i>Dockum</i>	<i>fluvial-deltaic and lacustrine clastics</i>		
<i>Permian</i>	<i>Ochoan</i>	<i>Dewey Lake</i>	<i>sandstone</i>	<i>Evaporite Confining System</i>	
		<i>Rustler</i>	<i>salt, anhydrite</i>		
		<i>Salado</i>	<i>salt</i>		
	<i>Guadalupian</i>	<i>Tansill</i>	<i>anhydrite</i>		
		<i>Yates</i>	<i>sandstone</i>		
		<i>Seven Rivers</i>	<i>anhydrite</i>		
		<i>Queen</i>	<i>sandstone</i>		
			<i>San Andres-Grayburg</i>		<i>dolomite-sandstone</i>
	<i>Leonardian</i>	<i>Clear Fork</i>	<i>limestone-dolomite</i>		
		<i>Wichita</i>			
<i>Wolfcampian</i>		<i>Wolfcamp</i>	<i>shelf limestones, minor shale</i>		
<i>Pennsylvanian</i>		<i>Cisco</i>			
		<i>Canyon</i>			
		<i>Strawn</i>			
		<i>Atokan</i>		<i>shale</i>	
		<i>Chester</i>			
<i>Mississippian</i>		<i>Mississippian Lime</i>	<i>limestone</i>	<i>Deep-Basin Brine Aquifer System</i>	
<i>Devonian</i>		<i>Woodford</i>	<i>shale</i>		
		<i>Devonian</i>	<i>limestone</i>		
<i>Silurian</i>		<i>Silurian</i>	<i>shale, limestone</i>		
<i>Ordovician</i>		<i>Montoya</i>	<i>limestone</i>		
		<i>Simpson</i>	<i>shale, limestone</i>		
		<i>Ellenburger</i>	<i>dolomite</i>		
<i>PRECAMBRIAN</i>			<i>igneous, metamorphic</i>	<i>Basement Aquiclude</i>	

Figure 21 (continued).

precipitated from formerly dissolved host materials. This is consistent with our observation that in the Happy Spraberry Field saddle dolomite is only present where the skeletal fragment content is high.

Dickson et al. (2001) invoked brine reflux as the main mechanism for the precipitation of saddle dolomite. They mention sulfate reduction in the reef material of the Wolfcampian Formation as an alternative to explain presence of pyrite.

Origin of brines and anhydrite

Stueber et al. (1998) studied formation waters in five formations of Devonian, Pennsylvanian and Early Permian in the Southwest Andrews area. The San Andres-Grayburg Formation (Lower Guadalupian) was deposited on top of the Clear Fork Formation. Its fluids exhibit moderate salinity (29-59 g/L). Fluids from the Wolfcampian Formation have much higher salinities (70-215 g/L) which is consistent with the salinity value in the Happy Spraberry Field (200 g/L from estimates from resistivity logs).

Geochemical data demonstrate that brines in Pennsylvanian-Wolfcampian shelf limestones in the Southwest Andrews area have undergone halite precipitation, indicating that these highly saline brines have descended more than 1000 meters as a result of fluid density differences (figure 22). The brines moved around or through strata that latter acted as seals. Because the same depositional configuration occurred in the Happy Spraberry Field, similar dissolution-precipitation processes could have happened in order to explain the presence of both anhydrite and the high brine salinity.

In the Southwest Andrews area, a much younger flow of low-salinity meteoric water from the Pecos River mixes with the high salinity brine (Stueber et al., 1998). This is shown by isotopic analyses on hydrogen and oxygen, and by a wide range of brine salinity. The formations are suspected to be highly compartmented because some parts are affected by the mix of brines and exhibit relatively low values of salinity, but other parts are not affected and exhibit high values of salinity. The homogeneous salinities measured in the wells of the Happy Spraberry Field do not indicate such a mixing.

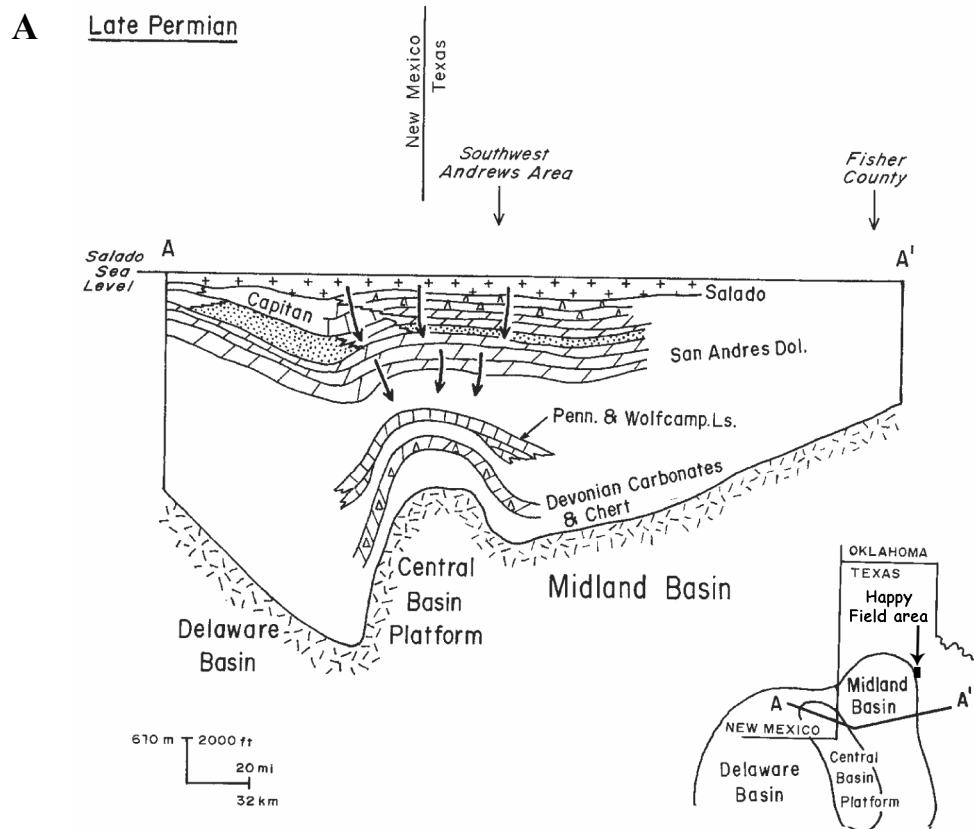


Figure 22. Highly schematic west-east cross sections throughout the Delaware and Midland Basins. A) Cross section during Salado deposition (Late Permian) showing descent of halite saturated brine that entered Pennsylvanian and Wolfcampian shelf limestones on the Central Basin platform. (B) Cross section showing suggested migration of brines of meteoric origin that began 5–10 m.y. ago and has reached Permian–Devonian carbonate strata on the Central Basin platform. (Modified after Stueber et al., 1998).

B Late Miocene - Present

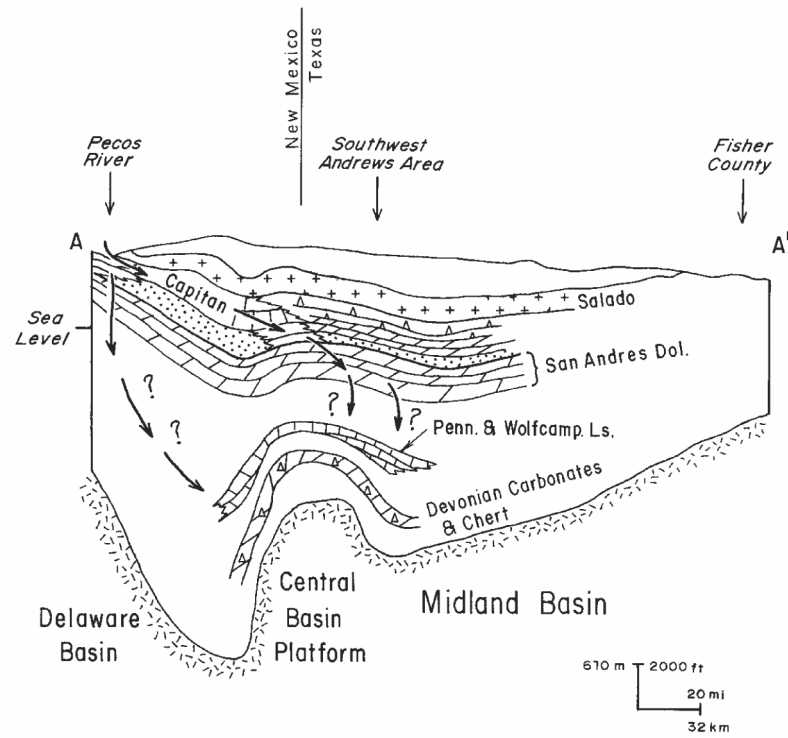


Figure 22 (continued).

POROSITY, PERMEABILITY AND WATER SATURATION

Porosity-permeability correlations

Hammel (1996) defined flow units of homogeneous porosity and permeability pair values in the Happy Spraberry Field but did not find a correlation between porosity and permeability. Laymann (2002) failed to find a correlation when considering all measurements without any classification in well 19-4.

Diagenesis was facies selective (dissolution) and its intensity varied between facies and within individual facies (especially in the oolitic grainstones). Thin section observation shows that depositional porosity in the oolitic grainstones was strongly modified during burial. Facies porosity and permeability are controlled not by depositional processes but by diagenesis, which shows a great variability. The same phenomena occurred in the oolitic packstones, which had lower compaction. A correlation between porosity and permeability may be easier to identify where diagenesis did not modify the pore system so much, as for example in the rudstones and bindstones.

Rudstones, bindstones and oolitic packstones

Cores from wells Lott 19-7 and Lott 19-8 exhibit thick intervals of rudstones and bindstones. The Lott 19-7 core consists mainly of mixed bindstones and rudstones with some oolitic packstones at the top. The core in Lott 19-8 is mainly rudstones interbedded with oolitic packstones. The ooid content in the rudstones is higher in Lott 19-8 than in Lott 19-7. As ooids are the most affected grains by diagenesis, a porosity-permeability correlation was experienced for the Lott 19-7 data first.

Non reservoir (shaly) intervals were identified on cores, thin sections, and logs. Permeability was plotted against porosity (figure 23). In the rudstones and bindstones there is a clear trend on the semi-log plot and the coefficient of determination is good ($R^2 = 0.62$). This type of correlation is well known and is expected in carbonates (Lucia,

1995). The oolitic packstones are on the same trend. The trend on the plot was computed using all reservoir facies.

Facies in the Lott 19-8 well have more ooids than in the Lott 19-7 well, but the ooid content is never above 50%. Shaly intervals were excluded and all other measurements were plotted on a semi-log graph (figure 24). A trend is also clearly identified ($R^2 = 0.65$) and it is very similar to the one in the Lott 19-7 well. Four measurements are clearly below the trend and are close to the shale group. A thin section cut from one of these samples is a more silty facies.

Oolitic grainstones and packstones

In the Lott 19-4 well laboratory measurements of porosity and permeability are available in oolitic grainstones/ packstones and rudstones. Plotting all measurements on the same graph shows that generally, permeability increases with porosity (Laymann, 2001). But a trend computed from the rudstone, packstone and grainstone facies would have a very coefficient of determination ($R^2 = 0.06$). Finer distinctions within facies have to be identified first.

Figure 25 shows a semi-log plot of permeability against porosity in well Lott 19-4. In the oolitic packstones and in the rudstones, the same trend ($R^2 = 0.66$) as in wells Lott 19-7 and Lott 19-8 is observed. In the oolitic grainstones, no trend can be identified but most of the samples exhibit permeability in the 1-15 mD range. An attempt to find a trend in the diagenetically deeply modified facies was done, but thin sections were not numerous enough to be conclusive on the existence of such a correlation.

Several thin sections in samples of oolitic grainstones were available, five of them in the 1-3 mD range. Two had high porosity (over 25%) and three had low porosity (below 20%). The high-porosity low-permeability samples are well cemented. Calcite cement is widespread in intergranular porosity, and compaction had little effect on porosity but molds are little connected and permeability is low. On the contrary, the low-porosity low-permeability samples contain well-connected fractured molds plugged by

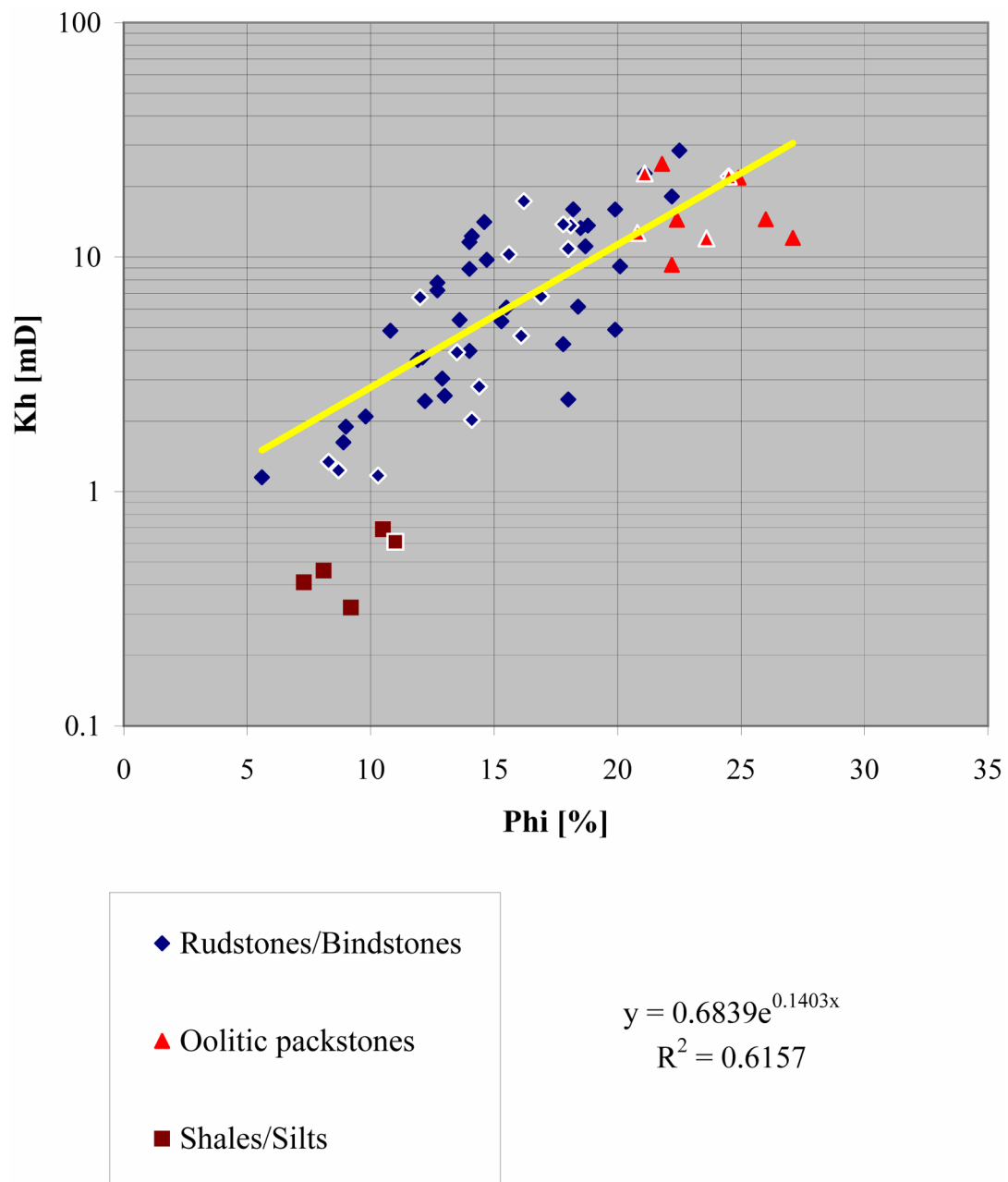


Figure 23. Well 19-7. Porosity-permeability semi-log cross plot. The trend is derived from the rudstone, bindstone and oolitic packstone facies. Samples where thin sections were cut are outlined in white.

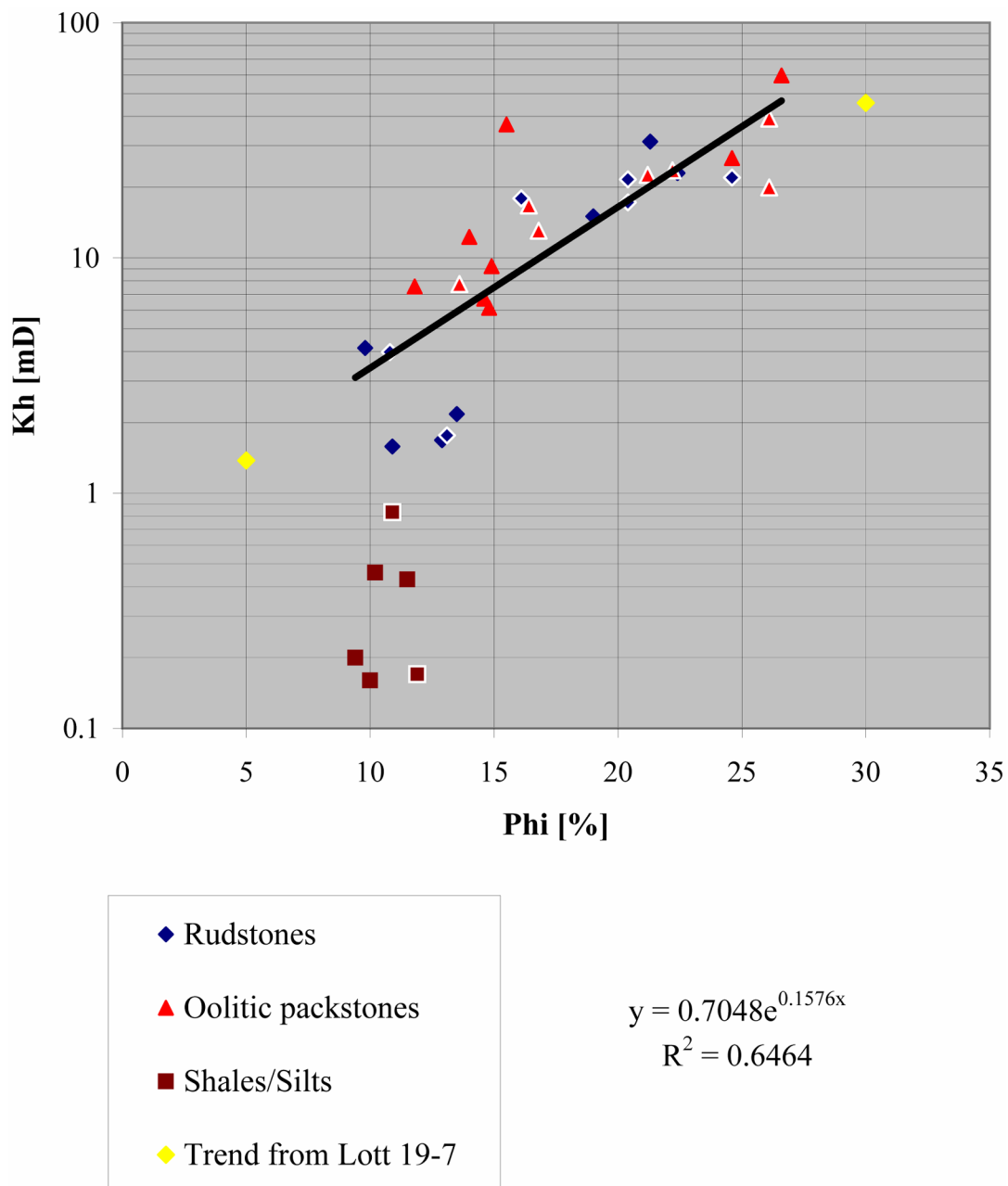


Figure 24. Well 19-8. Porosity-permeability semi-log cross plot. The trend is derived from the rudstone, bindstone and oolitic packstone facies. Samples where thin sections were cut are outlined in white.

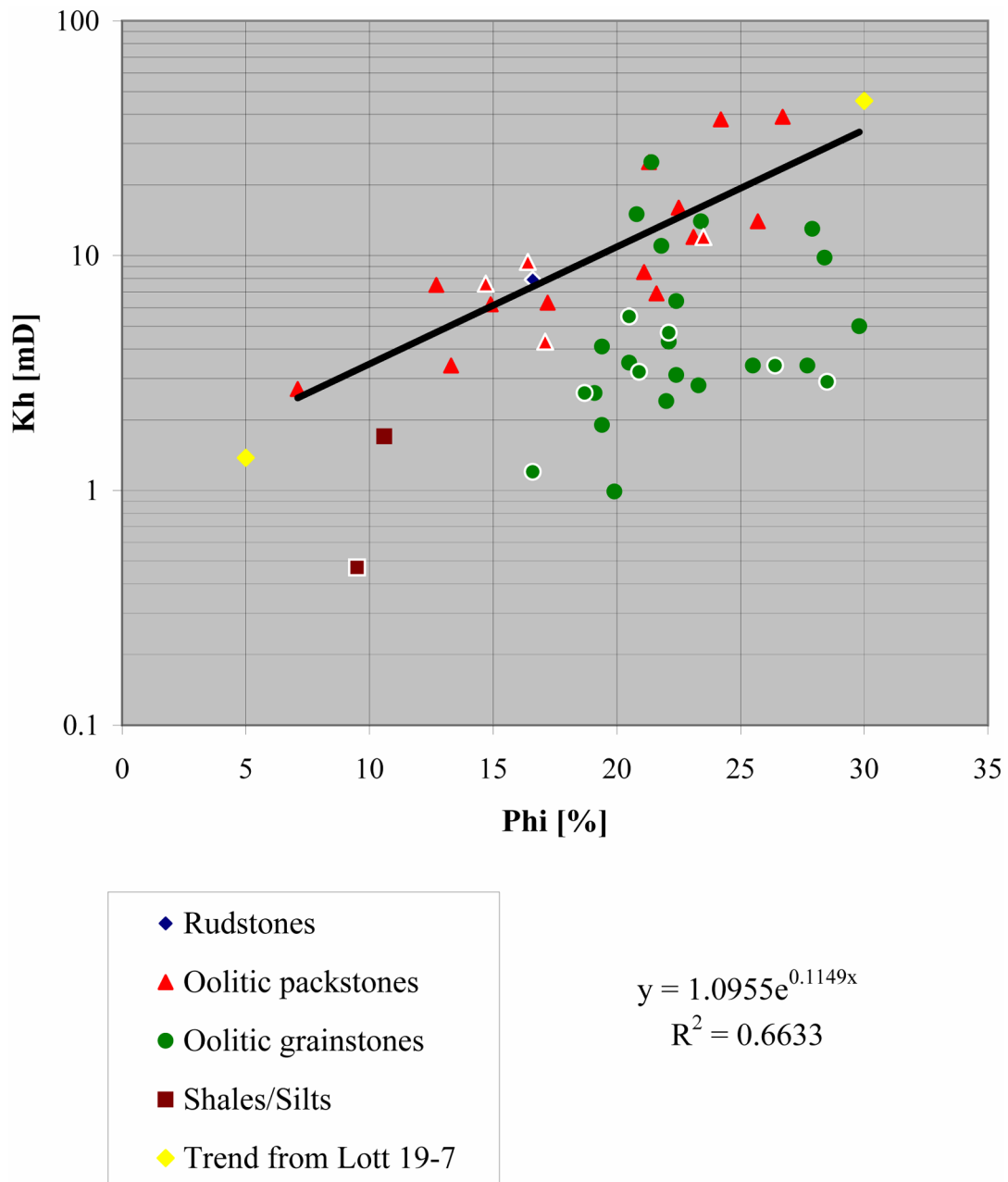


Figure 25. Well 19-4. Porosity-permeability semi-log cross plot. The trend is derived from the rudstone and oolitic packstone facies. Samples where thin sections were cut are outlined in white.

anhydrite Some of the facies interpreted as oolitic grainstones on cores are still on the trend defined from the other facies.

Discussion

In rudstones, bindstones and oolitic packstones (well Lott 19-7), a fair correlation exists between porosity and permeability. If the ooid content is increased in the rudstones (well Lott 19-8), porosity and permeability are still on the same trend. But in oolitic grainstones no trend was identified. Values of porosity and permeability in the oolitic grainstones are smaller than in the oolitic packstones that are the best reservoir rocks.

All the different facies at Happy Spraberry Field underwent the same sequences of diagenetic events, but the intensity of the phases was not the same in all reservoir zones. Grainstones and packstones were more affected by selective dissolution. In the grainstones, variability of calcite cement I precipitation induced a variability in compaction effects. The amount of anhydrite pore filling varies greatly in grainstones; therefore, diagenesis has been so intense and variable in the grainstones that depositional porosity is completely overprinted and no trend was identified on the porosity-permeability plot. In the other facies, where diagenesis was less intense and less variable, the correlation between porosity and permeability is still reliable. Because diagenetic boundaries follow facies boundaries, a lithofacies map can serve as a proxy for a depositional porosity map.

Even if original depositional porosity must have been greater in the oolitic grainstones, the complexity of diagenesis reduced their reservoir quality. In the oolitic packstones, neomorphosed mud protected moldic porosity from important collapses and anhydrite plugging.

In the rudstones, bindstones and oolitic packstones, the correlation shown in figure 26 should be used for well-log analysis and permeability prediction. Permeability in the oolitic grainstones can not be derived from porosity.

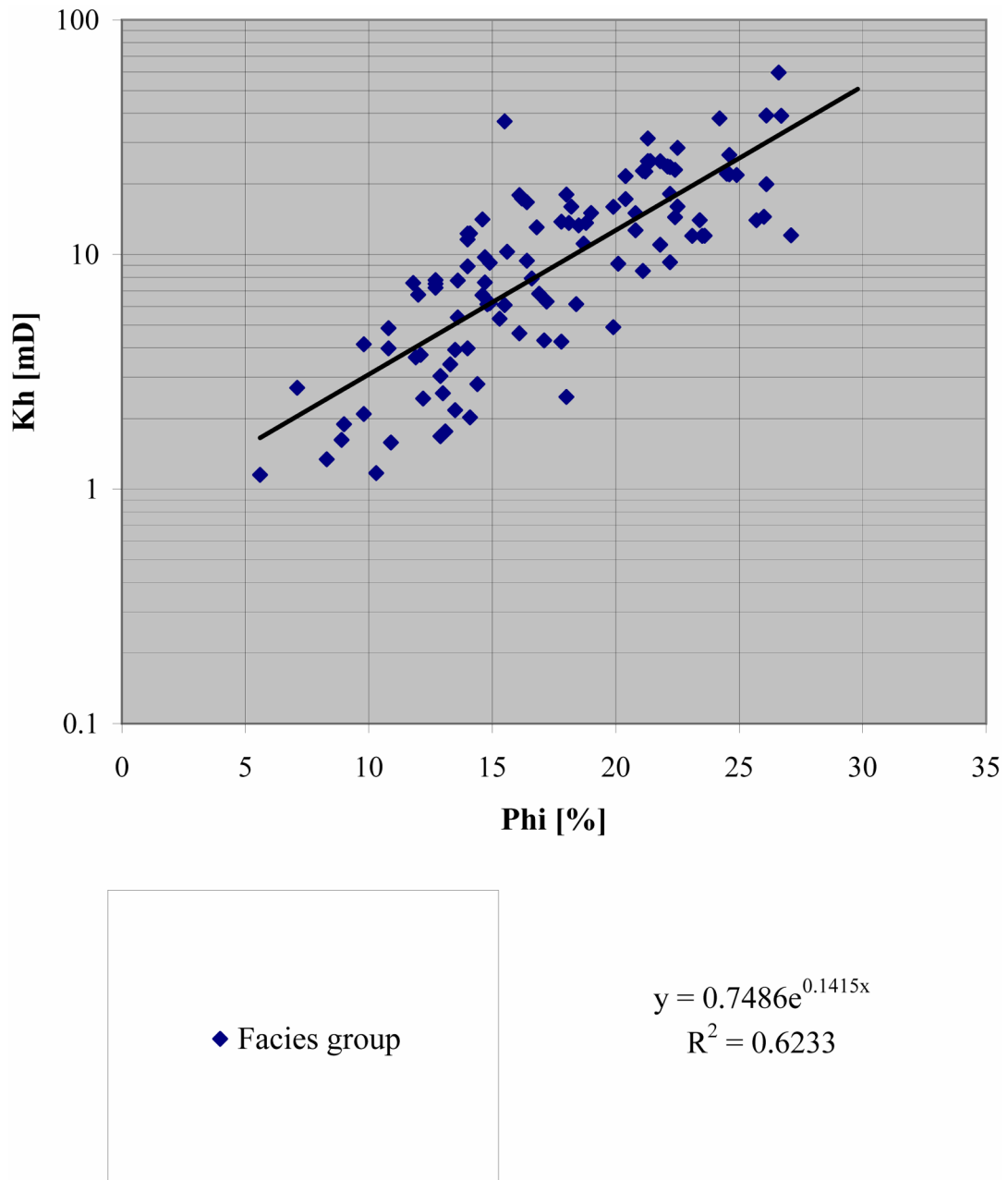


Figure 26. Porosity-permeability semi-log cross plot that groups all rudstone, bindstone and oolitic packstone facies of wells Lott 19-4, Lott 19-7 and Lott 19-8.

Previous studies by Hammel (1996) and Layman (2002) did not emphasize diagenesis and treated it as if all diagenetic alterations had a uniform effect on reservoir characteristics at Happy Spraberry Field. Their work did not focus on thin section study of diagenetic characteristics or the sequence of diagenetic events and how these characteristics influenced reservoir quality. For example, according to Layman (2002) “at Happy Field [...] a close correlation of porosity and permeability is non-existent”. The present study clearly shows that diagenesis has arguably had the most significant geological impact on reservoir quality at Happy Spraberry Field. Because diagenesis is also facies-selective, it is comparatively easy to identify boundaries of diagenetic influence because those influences follow depositional facies boundaries.

Saturation exponent and fluids saturation

Citing industry sources, Hammel (1996) notes that the original oil in place at Happy Spraberry Field is 17.2 MMBO. The present study utilized wireline logs for stratigraphic correlation but no attempts were made to calculate S_w to compute OOIP for comparison with Hammel’s figures. However, saturation calculations were at first attempted to determine whether calculated S_w values could be used in making such comparisons. S_w calculations are based on the Archie equation:

$$S_w^n = \frac{a}{\Phi^m} \cdot \frac{R_w}{R_t}$$

Where S_w is the initial water saturation, n is the saturation exponent, a is the tortuosity factor, Φ is the porosity, R_w is the formation water resistivity and R_t is the true formation resistivity.

Tortuosity and cementation factors

The tortuosity factor varies around 1 and does not have a strong influence on water saturation (Ahr, course notes). The commonly used value of 1 was then accepted in this study.

The cementation exponent has greater impact in Archie's formula because it is the exponent of the porosity. Moreover it varies over range of 1 to 5. Figure 27 from Focke and Munn (1987) was used to determine this parameter. Oolitic grainstones have an average porosity in the 20-25% range and most of it is well connected. Oolitic skeletal packstones exhibit lower porosities (15-20%) but are less connected (maximum 30% of porosity is not connected). Porosity in the rudstones and bindstones is wide in range but always well connected. An average cementation exponent was estimated to be 2, which is a classic value. Moreover, the variations in pore type in the oolitic grainstones are shorter-scale than the resolution of the logging tool. What is recorded is more an average medium connected moldic porosity.

Water resistivity

Wells Lott 19-4 and Lott 19-8 were drilled using a fresh water mud and resistivities were measured using a dual induction tool (medium and deep) and a laterolog (short guard). In case of a high resistivity mud, it is better to compute an "apparent formation water resistivity" (R_{wa}) in a water bearing zone than to use the SP signal to derive it. The Lott 19-7 well was drilled with a salt gel and log using a dual laterolog-MSFL tool. For consistency, the same method was used in well Lott 19-7 to compute the formation water resistivity. The laterolog short guard was corrected for borehole effect and the MSFL for the mudcake effect.

Results are summarized in Table 2 and give consistent values in the three wells which correspond to a salinity of about 170,000-200,000 ppm or 190-230 g/L.

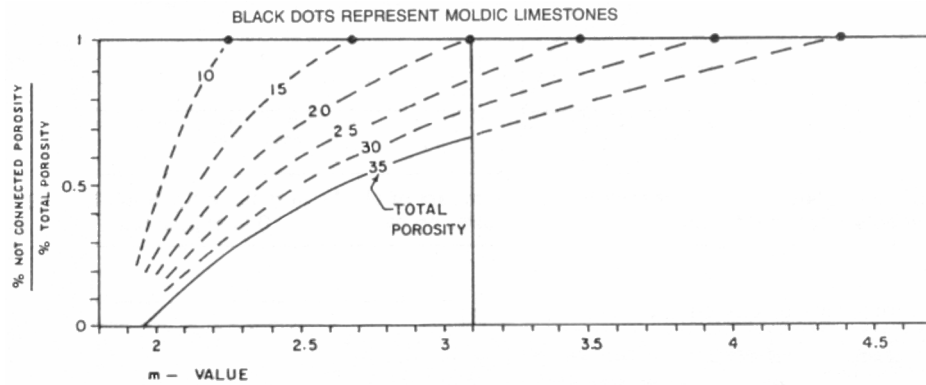


Figure 27. Effect of separate vug porosity on Archie “m”, or cementation exponent (after Focke and Munn, 1987).

Table 2. Apparent water resistivity computed in wells Lott 19-4, Lott 19-7 and Lott 19-8.

Well	Depth [ft]	Rwa ohm·m
Lott 19-4	5052	0.03
Lott 19-7	5055	0.038
Lott 19-8	5055	0.034

Saturation exponent

In the producing interval, porosity values used in Archie’s formula were from laboratory measurements; if such a measurement did not exist, porosity was derived from the spectral density and neutron logs. This study considered that the deep induction or the deep laterolog gave good estimates of the true formation resistivity.

The choice of the saturation exponent is critical because of its importance in Archie's formula. A commonly accepted range is 1.2-3.0 (Ahr, course notes) but much higher values are reported such as 25 in strongly oil-wet reservoir rocks (Hamada et al., 2001). It is suspected that the saturation exponent decreases when water saturation decreases. This saturation exponent can be derived if the water saturation is measured in a core of the oil bearing zone. When it is not known, usually a value of 2 is used.

As previously noted, none of the fluid saturations measured in the cores of Happy Spraberry Field were considered to be realistic representations. Because the saturation exponent could not be derived a value of 2 could have been used but the porosity-permeability model shows us that the oolitic grainstones have different petrophysical characteristics than the other facies. It is probable that they also had different saturation exponents.

Rather than computing initial water saturation, a range for the saturation exponent was derived using a probable initial water saturation of 10-15% in all facies. This was done in the three wells at different depths which were chosen in clear rudstones or bindstones without ooids, in oolitic grainstones and in oolitic packstones. Results are shown in table 3.

First almost all values are within the usually accepted range of 1.2-3. Some values are slightly lower in the rudstones and bindstones, but initial water saturation might be higher than 10% there. Second, the facies in the Happy Spraberry Field seem to exhibit different saturation exponent values following the same classification as for the porosity-permeability model. Bindstones/rudstones/oolitic packstones have a probable saturation exponent between 1.2 and 2. Oolitic grainstones have higher exponents between 2 and 3.

These computations do not give the value of the saturation exponent, neither the value of the initial water saturation. They only show that regarding n and S_w , two different behaviors exist depending on the facies (oolitic grainstones or oolitic packstones/ rudstones/bindstones).

Table 3. Computation of the saturation exponent “n”, given initial water saturation.

Well	Oolitic grainstones			Rudstones/Bindstones/Oolitic packstones		
	Depth [ft]	10% Assumed Sw	15% Assumed Sw	Depth [ft]	10% Assumed Sw	15% Assumed Sw
Lott 19-4	4916	2.1	2.55	4910	1.38	1.68
Lott 19-4	4925	2.54	3.09			
Lott 19-4	4935	2.21	2.68			
Lott 19-7				4934	1.04	1.26
Lott 19-7				4950	1.25	1.52
Lott 19-7				4975	0.93	1.13
Lott 19-8	4934	2.36	2.86	4906	1.54	1.87
Lott 19-8	4950	2.65	3.21	4990	1.21	1.46

CONCLUSIONS

1. Happy Spraberry Field produces from shallow-shelf oolitic grainstones/packstones and rudstones/bindstones of the Lower Clear Fork Formation trapped by siltstones and shales. The depositional environment was a shallow-marine distally-steepened ramp under tropical conditions.
2. Diagenesis includes four stages of calcite cementation, several occurrences of dissolution, mechanical compaction, anhydrite and saddle dolomite precipitation and chalcedony replacement. Bacterial sulfate reduction of the oil is suspected.
3. Diagenesis has been selective (dissolution of the ooid grains), intense (moldic porosity) and variable. Grainstones are the most affected facies where depositional porosity is overprinted by diagenesis.
4. A porosity-permeability correlation was derived with a good coefficient of determination ($R^2 = 0.62$) on semi-log plot in the rudstone, bindstone and oolitic packstone facies. No trend was observed in the oolitic grainstones.
5. The impact of diagenesis on depositional porosity can be variable. Previous workers on Happy Spraberry Field (Hammel, 1996; Layman, 2002) considered that the overprint of diagenesis on reservoir rocks was too strong to find a fair correlation between porosity and permeability. This study shows that a closer look on diagenetic processes and variability allows identifying reservoir zones where a correlation is still available.
6. Oolitic grainstones may have different saturation exponent than the other facies.

REFERENCES CITED

- Adams, J.E., H.N. Frenzel, M.L. Rhodes, and D.P. Johnson, 1951, Starved Pennsylvanian Midland Basin: AAPG Bulletin, v. 35, p. 2600-2607.
- Ahr, W.M., and B.S. Hammel, 1999, Identification and mapping of flow units in carbonate reservoirs; an example from the Happy (Spraberry) Field, Garza County, Texas: Energy Exploration and Exploitation, v. 17, p. 311-334.
- Asserto, R., and R.L. Folk, 1980, Diagenetic fabrics of aragonite, calcite, and dolomite in ancient peritidal-spelean environments: Triassic Calcarea Rosso, Lombardia, Italy: Journal of Sedimentary Geology, v. 50, p 371-394.
- Atchley, S.C., M.G. Kozar, and L.A. Yose, 1999, A predictive model for reservoir distribution in the Permian (Leonardian) Clear Fork and Glorieta formations, Robertson Field area, West Texas: AAPG Bulletin v. 83, p.1031-1056.
- Chow, N., and N.P. James, 1987, Facies-specific, calcitic and bimineralic ooids from Middle and Upper Cambrian platform carbonates, Western Newfoundland, Canada: Journal of Sedimentary Petrology, v. 57, p. 907-921.
- Collins, J.A., and L. Smith, 1975, Zinc deposits related to diagenesis and intrakarstic sedimentation in the Lower Ordovician St George Formation, Western Newfoundland: Bulletin of Canadian Petroleum Geology, v.27, p. 393-427.
- Dickson, J.A.D., L.P. Montañez, and A.H. Saller, 2001, Hypersaline burial diagenesis delineated by component isotopic analysis, Late Paleozoic limestones, West Texas: Journal of Sedimentary Research, v. 71, p. 372-379.
- Dunham, R. J., 1962, Classification of carbonate rocks according to depositional texture, *in* W. E. Ham, ed., Classification of carbonate rocks-a symposium: AAPG Memoir 1, p. 108-121.
- Focke, J.W., and D. Munn, 1987, Cementation exponents in Middle Eastern carbonate reservoirs: SPE Formation Evaluation, v. 2, p. 155-167.
- Guevera, E.H., 1988, Geological characterization of Permian submarine fan reservoirs of the Driver Waterflood Unit, Spraberry Trend, Midland Basin: Texas Bureau of

Economic Geology, University of Texas-Austin, Report of investigation No. 172, 44 p.

Hamada, G.M., M.N. Al-Awad, and Alsughayer, 2002, Variable saturation exponent effect on the determination of hydrocarbon saturation: SPE Asia Pacific Oil and Gas Conference and Exhibition, Melbourne, Australia, 8-10 October 2002, 19 p.

Hammel, B.S., 1996, High resolution reservoir characterization of the Permian (upper Leonardian) Spraberry formation, Happy Spraberry Field, Garza County, Texas: Unpublished Master's Thesis, Texas A&M University, 1996, 157 p.

Handford, C.R., 1981, Sedimentology and genetic stratigraphy of Dean and Spraberry Formations (Permian), Midland Basin, Texas: AAPG Bulletin, v. 65, p. 1602-1616.

Heydari, E., R.D. Snelling, W.C. Dawson, and M.L. Machin, 1993, Ooid mineralogy and diagenesis of the Pitkin formation, North-Central Arkansas, *in* Mississippian Oolites and Modern Analogs, AAPG Special Publication, p. 175-184.

Hills, J.M., 1985, Structural evolution of the Permian basin of West Texas and New Mexico, *in* P.A. Dickerson and W.R. Muehlberger, eds., Structure and tectonics of trans-Pecos Texas: West Texas Geological Society Field Conference, publication 85-81, p. 89-99.

Land L.S., E.W. Behrens, and S.A. Frishman, 1979, The ooids of Baffin Bay, Texas: Journal of Sedimentary Geology, v.47, p. 1269-1298.

Layman, J.M., 2002, Porosity characterization utilizing petrographic image analysis: implications for identifying and ranking reservoir flow units, Happy Spraberry Field, Garza County, Texas: Unpublished Master's Thesis, Texas A&M University, 2002, 99 p.

Lucia, F.J., 1995, Rock-fabric/petrophysical classification of carbonate pore space for reservoir characterization: AAPG Bulletin, v. 79, p. 1275-1300.

Machel, H.-G., 1987, Saddle dolomite as a by-product of chemical compaction and thermochemical sulphate reduction: Geology, v. 15, p. 936-940.

Machel, H.-G., 2001, Bacterial and thermochemical sulphate reduction in diagenetic settings – old and new insights: Sedimentary Geology, v. 140, p. 143-175.

- Mazzullo, S. J., 1995, Permian stratigraphy and facies, Permian Basin (Texas-New Mexico) and adjoining areas in the mid-continent United States, *in* P.A. Scholle, T.M. Peryt, and D.S. Ulmer-Scholle, eds., *The Permian of Northern Pangea: Sedimentary Basins and Economics Resources*, Springer Verlag, New York, v. 2, p. 40.
- Mazzullo, S. J., and A. M. Reid II, 1989, Lower Permian platform and basin depositional systems, northern Midland Basin, TX, *in* P.D. Crevello, J.L. Wilson, J.F. Sarg, and J.F. Read, eds., *Controls on carbonate platform and basin development: SEPM Special Publication No. 44*, p. 305-320.
- Montgomery, S.L., and W.H. Dixon, 1998, New depositional model improves outlook for Clear Fork infill drilling: *Oil and Gas Journal*, v. 96, p. 94-98.
- Moore, C.H., 2001, Carbonate reservoirs, porosity evolution and diagenesis in a sequence stratigraphic framework: *Developments in Sedimentology* 55, 444p.
- Morrow, D.W., G.L. Cumming, and R.B. Koepnick, 1986, Manetoe facies – a gas-bearing, megacrystalline, Devonian dolomite, Yukon and Northwest territories, Canada: *AAPG Bulletin*, v. 70, p. 702-720.
- Pratt, B.R., 2001, Oceanography, bathymetry and syndepositional tectonics of a Precambrian intracratonic basin: integrating sediments, storms, earthquakes and tsunamis in the Belt Supergroup (Helena Formation, ca. 1.45 Ga), western North America: *Sedimentary Geology* v. 141-142, p. 371-394.
- Ross, C.A., 1986, Paleozoic evolution of southern margin of Permian Basin: *Geological Society of America Bulletin*, v. 97, p. 536-554.
- Sano H., K. Horibo and Y. Kumamoto, 1990, Tubiphytes-Archaeolithoporella-Girvanella reefal facies in Permian buildup, Mino terrane, central Japan: *Sedimentary Geology*, v. 68, p. 293-306.
- Stueber, A.M., A.H. Saller, and H. Ishida, 1998, Origin, migration, and mixing of brines in the Permian Basin: geochemical evidence from the Eastern Central Basin Platform, Texas: *AAPG Bulletin*, v. 82, p. 1652-1672.
- Tucker, M.E., 1984, Calcitic, aragonitic and mixed calcitic-aragonitic ooids from the mid-Proterozoic Belt Supergroup, Montana: *Sedimentology*, v. 31, p. 627-644.

- Tucker, M.E., 1990, Diagenetic processes, products and environments, *in* M.E. Tucker and V.P. Wright, eds., Carbonate sedimentology, Blackwell Science Ltd, Oxford, p 314-364.
- Ward, R.F., C.G. Kendall, and P.M. Harris, 1986, Upper Permian (Guadalupian) facies and their association with hydrocarbon-Permian basin, West Texas and New Mexico: AAPG Bulletin, v. 60, p. 239-262.
- Wilkinson, B.H. and E. Landing, 1978, "Eggshell digenesis" and primary radial fabric in calcite ooids: Journal of Sedimentary Petrology, v. 48, p. 1129-1138.
- Yang, K.M., and S.L. Dorobek, 1994, The Permian Basin of West Texas and New Mexico: tectonic history of a "composite" foreland basin and its effect on stratigraphic development, *in* S.L. Dorobek and G.M. Ross, eds., Stratigraphic Evolution of Foreland Basins: SEPM Special Publication 52, p. 147-172.

APPENDIX

Three spreadsheets will be found in this annex. They show the repartition of the diagenetic features in the thin sections. Occurrences were not accurately counted but visually estimated. The following abbreviations are used: T = traces, R = rare, C = common, A = abundant, OGST = oolitic grainstone, OPST = oolitic grainstone, RDST = rudstone, BDST = bindstone, FLST = floatstone, ShSST = shaly sandstone, SiST = Siltstone.

VITA

Name:

Vincent Philippe Guillaume MAZINGUE-DESAILLY

Permanent Address:

32 rue Clemenceau

76 130 Mont Saint Aignan, FRANCE

Education:

Ingénieur des Mines, 2002

Ecole Nationale Supérieure des Mines de Paris

Paris, FRANCE

M.S., Geology, 2004

Texas A&M University

College Station, Texas